

Exploring the Metabolic Profiling and Anticancer Activities of Red Sea Sponges *Echinodictyum asperum* and *Callyspongia siphonella* against Human Breast Cancer Cells: A Comparative Study

Samah S. Abuzahrah,[#] Tahani Bakhsh, Reham Hassan Mekky,^{*} Serag Eldin I. Elbehairi, and Nouf Juaid[#]



Cite This: *ACS Omega* 2025, 10, 9402–9425



Read Online

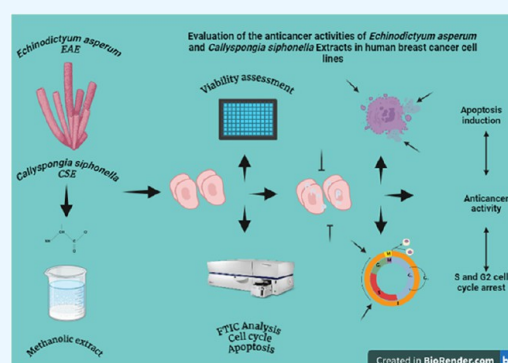
ACCESS |

Metrics & More

Article Recommendations

Supporting Information

ABSTRACT: Marine sponges are noteworthy sources of bioactive secondary metabolites that demonstrate fundamental functions in defense mechanisms and ecological interactions. This study focused on the extraction and characterization of metabolites from two sponge species, *Echinodictyum asperum* and *Callyspongia siphonella*, obtained from the Red Sea coast of Saudi Arabia. Methanol extraction generated EAE and CSE extracts, which were subjected to metabolic profiling, illuminating 44 identified metabolites involving fatty acids, sterols, terpenoids, long-chain amides, and alkaloids. The cytotoxic effects of both were assessed versus MDA-MB-231 and MCF-7 breast cancer cell lines, utilizing the sulforhodamine B (SRB) assay, with IC₅₀ values of about 2.7 $\mu\text{g}/\text{mL}$ for CSE and 0.5 $\mu\text{g}/\text{mL}$ for EAE on MCF-7 cells and 8.7 $\mu\text{g}/\text{mL}$ for EAE and 45.3 $\mu\text{g}/\text{mL}$ for CSE on MDA-MB-231 cells. Flow cytometry analysis indicated that both extracts induced apoptosis and necrosis across cell lines. Particularly, EAE induced the G2 phase arrest in MCF-7 cells, while CSE elevated the S phase population in both cell lines. As well, CSE boosted autophagy especially in MDA-MB-231 cells. Comparative analyses with the existing literature underscore the therapeutic potential of these sponge-derived metabolites in cancer medication. Molecular docking studies demonstrated robust binding affinities between selected metabolites and key targets involving MCL-1, BCL-2, and ER α . In conclusion, this research emphasizes the significant cytotoxic features of EAE and CSE extracts, proposing their potential purposes in cancer treatment via distinct mechanisms of action.



1. INTRODUCTION

Breast cancer has surpassed other cancers in terms of the number of patients diagnosed with the disease since the year 2020.¹ Despite the fact that chemotherapeutic medicines for the treatment of breast cancer are readily available, which have greatly improved patient welfare and survival rates, a large number of patients continue to pass away on a yearly basis due to metastases and drug resistance.² For this reason, it is still of the utmost importance to find new treatments that are effective against breast cancer in order to eradicate this disease.³ Marine organisms offer a wide variety of natural compounds that are absolutely one of a kind and demonstrate considerable pharmacological effects. Several of these items are now being tested in either preclinical or clinical trials.^{4,5}

Porifera, often known as sponges, are a species that is primarily found in marine environments, specifically in the coastal and abyssal zones of the ocean.⁶ There are over 8500 species of sponges that have been described by scientists all over the world.⁶ In terms of natural marine products, sponges are considered to be the most prolific source, as they are responsible for 30 percent of all products that have been identified. Marine sponges, as sessile invertebrates, generate a diverse range of metabolites that are important for environmental adaptation and

self-preservation. These natural products involve different chemical classes such as rare nucleosides, sterols, cyclic peptides, bioactive terpenes, alkaloids, peroxides, fatty acids, and halogenated amino acid derivatives. Sponge-derived bioactive compounds demonstrate several biological impacts, including antiviral, antioxidant, antiobesity, antihypertensive, antidiabetic, anticancer, and antiproliferative properties.^{5,7} Sponge bioactive compounds have been shown to have anticancer and antiproliferative properties. The anticancer potential of metabolites generated from marine sponges is related to several different cellular and molecular pathways. These pathways include the suppression of growth, the induction of apoptosis and autophagy, the inhibition of migration, and the antiangiogenic actions.^{5,8}

Echinodictyum asperum belongs to the phylum Porifera, class Demospongiae, order Axinellida, and family Raspailiidae. This

Received: November 9, 2024

Revised: February 5, 2025

Accepted: February 11, 2025

Published: February 25, 2025



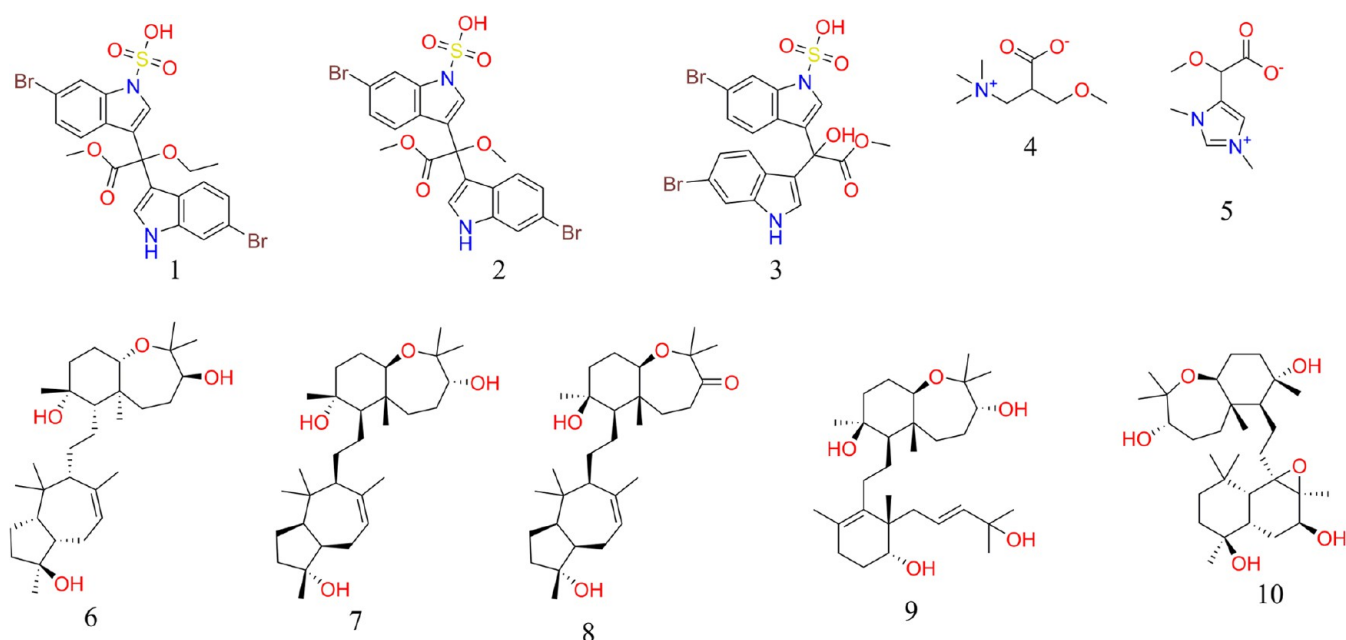


Figure 1. Structures of compounds previously isolated from *E. asperum* and *Callyspongia siphonella*: (1) echinosulfonic acid A, (2) echinosulfonic acid B, (3) echinosulfonic acid C, (4) echinobetaine A, (5) echinobetaine B, (6) sipholenol A, (7) sipholenol B, (8) sipholenone A, (9) siphoenllinol C, and (10) sipholenol I.

species falls under the subfamily Echinodictyinae and genus *Echinodictyum*.⁹ *E. asperum* was first described by H. Ridley and Arthur Dendy in 1886.¹⁰ A little information is available regarding the active constituents of *Echinodictyum*. In this sense, ref 11 isolated the antibacterial bromindole sulfonic acids, echinosulfonic acids A–C as well as the sulfone echinosulfone A from the southern Australian *Echinodictyum* sp. Furthermore, ref 12 isolated two nematocidal betaines, echinobetaine A and B (Figure 1).

C. siphonella is a species of marine sponge within the phylum Porifera, class Demospongiae, order Haplosclerida, and family Callyspongiidae.¹³

Marine sponges, including the genus *Callyspongia*, are prolific producers of a variety of secondary metabolites with significant biological activities. These compounds are chemical defenses against predators, pathogens, and fouling organisms. Secondary metabolites identified in *C. siphonella* include alkaloids, terpenoids, polyacetylenes, polyketides, and peptides, which exhibit strong antimicrobial and antifungal properties, anti-inflammatory, cytotoxic activities, and antiviral effects.^{14,15}

In this context, the secondary metabolites of *C. siphonella* have shown considerable promise in anticancer research. Sipholane triterpenoids (sipholenol A and B) exhibited potent cytotoxicity against various cancer cell lines, including leukemia and breast cancer cells.¹⁶ They induced apoptosis by activating caspases and disrupting mitochondrial function, leading to cell death. Furthermore, they inhibited cell proliferation by interfering with cell cycle progression.¹⁶

Moreover, sipholane triterpenoids, viz., sipholenol A, sipholenone A, siphoenllinol C, and sipholenol I, exhibited cytotoxic activity and were able to reverse P-glycoprotein-mediated multidrug resistance (MDR) to colchicine with a predominance of sipholenol A, which increased the sensitivity of resistant KB-C2 cells to colchicine by 16 times¹⁷ (Figure 1).

In addition to inducing apoptosis, *C. siphonella* metabolites have been found to inhibit cell proliferation. This is achieved through various mechanisms, such as interfering with the cell

cycle progression. Some metabolites can halt cancer cells at specific cell cycle phases, preventing them from dividing and multiplying. This inhibition of cell cycle progression is crucial for controlling the growth of cancer cells and can be a powerful strategy for cancer therapy.^{15,18,19}

This study aimed to conduct untargeted metabolic profiling and evaluate the potential anticancer properties of methanol-based extracts from the Red Sea sponges *E. asperum* and *C. siphonella*. Specifically, the study aimed to assess the extracts' antiproliferative, proapoptotic, and antimigratory effects on human breast cancer cell lines MCF-7 and MDA-MB-231. In order to investigate the mechanisms that underlie these effects, a virtual screening was conducted on the primary constituents identified through reverse phase high-performance liquid chromatography-mass spectrometry (RP-HPLC-MS) and MS/MS, with doxorubicin serving as a positive control. The screening was focused on three breast cancer-associated antiapoptotic proteins.

2. MATERIALS AND METHODS

2.1. Sponge Material. The colonial tube-sponge material of *E. asperum* and *C. siphonella* was collected at a depth of 15–20 m by scuba diving from Jeddah on the Red Sea coast of Saudi Arabia (21° 42' 37.67" N 38° 59' 21.54" E) in October 2023. This species was collected and identified by Kamal Al-Dahoody, Faculty of Maritime Studies, King Abdulaziz University (KAU) Jeddah, Saudi Arabia. Voucher specimens (EAS and CSS) were deposited at the Department of Biological Sciences, College of Science, University of Jeddah, Jeddah P.O. Box 21959, Saudi Arabia.

2.2. Extraction and Isolation. The freeze-dried sponge material (*E. asperum* 243.0 g and *C. siphonella* 259.3 g) was minced and extracted exhaustively with a mixture of *n*-hexane/dichloromethane/MeOH (1:1:1, v/v) (3 × 2.5 L, three times). The combined extracts were concentrated under reduced pressure until dryness to yield a viscous dark brown oily material (12.5 and 11.7 g, respectively). The extract from *E.*

asperum was designated as EAE, while the extract from *C. siphonella* was designated as CSE.²⁰

2.3. RP-HPLC-MS/MS Analysis of EAE and CSE. The analyses were conducted by using an Agilent 1200 series quick resolution system (Agilent Technologies, Santa Clara, CA) that included a quaternary pump (G7104C) and an autosampler (G7129A). The volume of the injection was 5 μ L. The substances were isolated using a Poroshell 120 HiLiC Plus column (150 mm \times 3 mm, 2.7 μ m particle size, Agilent Technologies) with a flow rate of 0.3 mL/min.²¹ The system was connected to a 6530 Agilent Ultra-High-Definition (UHD) Accurate-Mass Q-TOF LC/MS (Palo Alto, CA) that had an electrospray (ESI) interface. The system was configured to operate in negative and positive ionization modes.²² The data analysis was performed using MassHunter Qualitative Analysis B.06.00 (Agilent Technologies) software. This analysis involved generating potential molecular formulas and observing retention times (RTs), molecular ion peaks (m/z), and fragmentation patterns. The data was then compared with the Reaxys database (<https://www.reaxys.com>, accessed on 1st July 2024²³) and the MarinLit database (<https://marinlit.rsc.org>, accessed on 1st July 2024¹³). In addition, the relevant literature was accessed from the Egyptian Knowledge Bank (<https://www.ekb.eg>, accessed on 1st July 2024).^{3,24,25}

2.4. Cell Lines. MCF-7 and MDA-MB-231 cell lines were provided by the American Type Culture Collection (ATCC, Boston, MA). RPMI 1640 medium supplemented with 10% fetal bovine serum and 100 IU/mL of PS (penicillin/streptomycin) was used to culture MCF-7 and MDA-MB-231 cell lines.

2.5. Cell Viability Assay. The cytotoxicity of sponge extract derivatives EAE and CSE was assessed using sulforhodamine B (SRB) assay. MCF-7 and MDA-MB-231 cells were seeded in 96-well plates at a density of 2000 cells per well and allowed to adhere for 24 h. The cells were then treated with varying concentrations of the sponge materials (0, 0.01, 0.1, 1, 10, and 100 μ g/mL) and incubated for 72 h at 37 $^{\circ}$ C. After the incubation period, the culture media were replaced with 10% trichloroacetic acid (TCA), and the cells were incubated for 1 h at 4 $^{\circ}$ C. The cells were then washed five times with distilled water and stained with 0.04% w/v sulforhodamine B (SRB) solution for 10 min at 25 $^{\circ}$ C in the dark. The excess stain was washed away with 1% acetic acid, and a 10 mM tris base solution was added to each well to dissolve the protein-bound dye. The optical density was then measured by using a microplate reader set at 540 nm. The IC₅₀ values, which represent the concentration of the sponge materials that inhibit 50% of the cell viability, were calculated using GraphPad Prism software. Dose–response curves were generated by plotting the viability % against the compound concentrations, allowing for the interpolation of the IC₅₀ values.

2.6. Cell Cycle Analysis. Human breast adenocarcinoma cells (MCF-7, MDA-MB-231) were seeded in a 6-well plate and allowed to adhere for 24 h. The cells were then treated with the previously calculated IC₅₀ concentrations of EAE and CSE and incubated for an additional 48 h. After the incubation period, the cells were trypsinized, harvested, and fixed in ice-cold 60% ethanol at 4 $^{\circ}$ C for 1 h. The cells were then washed twice with 1 \times PBS. Following the washing steps, the cells were stained with 100 μ L of propidium iodide (PI) solution containing RNase (Cell Signaling Technology; Boston, MA). The cells were incubated for 15 min in the dark and then washed twice with 1 \times PBS. Finally, flow cytometric analysis was performed using a Cytek Northern Lights (NL-2000) spectral flow cytometer

(Cytek Biosciences, Bethesda, MD) equipped with SpectroFlo Software version 2.2.0.3.

2.7. Apoptosis/Necrosis Analysis. MCF-7 and MDA-MB-231 cells (1×10^5) were cultured in a 6-well plate and incubated for 24 h at 37 $^{\circ}$ C. The cultured cells were then treated with the previously determined IC₅₀ concentrations of EAE and CSE and further incubated for 48 h. Untreated cells were used as a control. After the treatment period, the cells were trypsinized and washed twice with phosphate-buffered saline (PBS). Apoptosis assessment was then performed using an FITC Annexin V Apoptosis Detection Kit with PI (BioLegend; San Diego, U.K.), following the manufacturer's instructions. Briefly, the cell pellets were resuspended in 400 μ L of binding buffer and stained with a solution containing 10 μ L of PI and 5 μ L of FITC Annexin V. Additionally, reference groups were prepared, including unstained cells, cells stained with PI only, and cells stained with Annexin V-FITC only. The staining was done by gentle mixing for 15 min at room temperature in the dark. Finally, the cellular apoptosis and necrosis were evaluated using a Cytek Northern Lights (NL-2000) spectral flow cytometer equipped with SpectroFlo Software version 2.2.0.3.

2.8. Cell Autophagy Assay. MCF-7 and MDA-MB-231 cells were seeded into 6-well plates and treated with the previously calculated IC₅₀ concentrations of EAE and CSE. After 48 h of treatment, the cells were washed twice with PBS and then incubated with 1 μ g/mL of acridine orange dissolved in PBS for 15 min at 37 $^{\circ}$ C in a dark area. Acridine orange is a dye that selectively labels acidic vesicular organelles (AVOs), which are indicative of autophagic activity. The staining procedure involved incubating the cells with the dye, followed by washing to remove any excess stain. The stained cells were then analyzed using a Cytek Northern Lights (NL-2000) spectral flow cytometer equipped with SpectroFlo Software version 2.2.0.3. This allowed for the identification and quantification of the AVOs, which provided an assessment of the autophagic activity in the MCF-7 and MDA-MB-231 cell lines after treatment with EAE and CSE.

2.9. Molecular Docking. In vitro studies demonstrated that both *E. asperum* and *C. siphonella* exhibit significant inhibitory effects on breast cancer (BC) cell lines, indicating their potential as therapeutic agents for impeding BC tumor growth and proliferation. To explore the mechanisms underlying these effects, a virtual screening was performed on the major constituents identified via RP-HPLC-MS and MS/MS, alongside doxorubicin as a positive control, targeting three breast cancer-associated antiapoptotic proteins (see Table S1 for constituent details).

In breast cancer, antiapoptotic proteins such as BCL-2, MCL-1, and estrogen receptor α (ER α) play critical roles in tumor growth by inhibiting apoptosis, particularly in estrogen receptor-positive tumors. BCL-2, a well-known antiapoptotic protein, is frequently overexpressed in breast cancer and is linked to poor prognosis across various cancer types (Adams and Cory, 2018). MCL-1, another key regulator of apoptosis, promotes cancer cell survival and contributes to chemoresistance when overexpressed.²⁶ ER α , a transcription factor activated by estrogen binding, regulates gene expression that promotes cell proliferation, making it a crucial target in hormone-positive breast cancers.²⁷ Due to their roles in promoting cancer cell survival, these proteins are viable therapeutic targets, with drugs designed to inhibit their function in the treatment of breast cancer.

The three-dimensional (3D) structures of the target proteins—BCL-2 (PDB ID: 4MAN), MCL-1 (PDB ID:

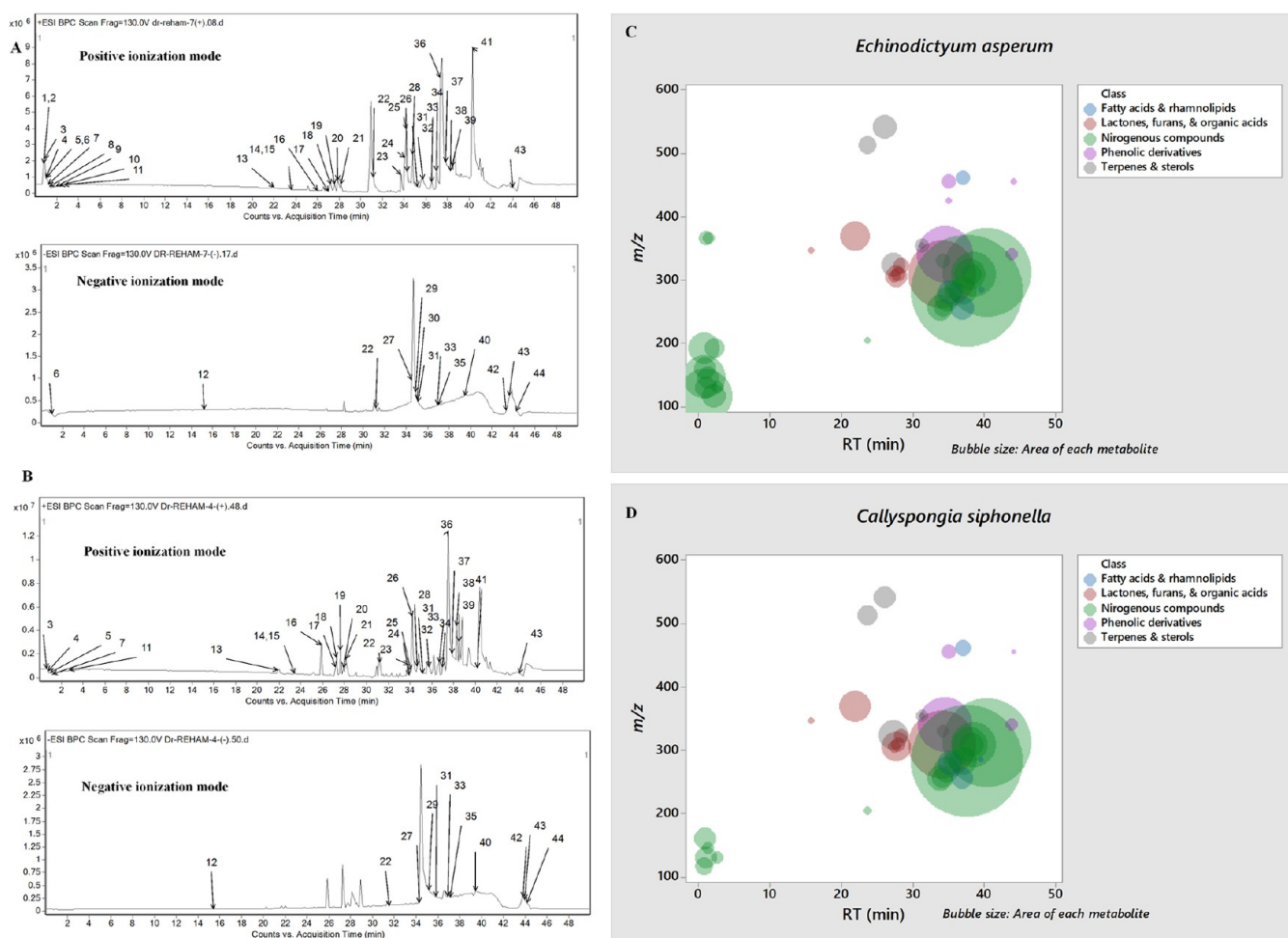


Figure 2. Base peak chromatograms (BPCs) in the positive and negative ionization modes of (A) *E. asperum* (EAE) and (B) *C. siphonella* (CSE) and bubble plots of the observed masses vs the retention time in relation to metabolite classes for (C) EAE and (D) CSE.

SFD0), and ER α (PDB ID: 1G50)—were retrieved from the Protein Data Bank (PDB) (<http://www.rcsb.org/structure>).²⁸ Protein preparation involved the removal of water molecules and the addition of polar hydrogen atoms using AutoDockTools (ADT), as described by Huey, Morris, and Forli.²⁹ Partial charges were assigned using the Marsili–Gasteiger method,³⁰ and the receptor structures were minimized using the Kollman united-atom force field, and then saved in a PDBQT format for docking.

Ligand preparation included the cocrystallized ligands (negative controls for validation), the constituents of the extracts, and doxorubicin (positive control). Ligands were drawn in ChemSketch, and geometries were optimized using AutoDock 4.2.³¹ Conversion to the PDBQT format was achieved through the prepare_ligand4.py script in ADT.

Docking simulations were performed using the Lamarckian genetic algorithm, with a grid box centered on the cocrystallized ligand-binding sites, set at dimensions of 40 Å in each direction (x , y , z). Parameters included 2,500,000 energy evaluations, 100 independent runs, and a population size of 150.³² Docking results were evaluated based on binding free energies, and conformations with energies within 3 kcal/mol of the lowest energy state were selected for further analysis. Additionally, docking was extended across all protein pockets to identify potential allosteric binding sites. Molecular interactions were

visualized by using BIOVIA Discovery Studio Visualizer 2021 to generate 2D interaction diagrams.

2.10. Statistical Analysis. All experiments were conducted in triplicate, and the results were reported as mean \pm standard deviation (SD). Student's t -test and one-way analysis of variance (ANOVA) were adopted to evaluate statistical significance using GraphPad prism (version 7). P values <0.05 were regarded as statistically significant. Microsoft Excel 365 (Redmond, WA) was used for conditional formatting, and Minitab 17 (Minitab, Inc.) was used for bubble plots.

3. RESULTS


3.1. Metabolite Characterization by LC–MS and MS/MS of *E. asperum* and *C. siphonella*. The metabolic profiling of *E. asperum* and *C. siphonella* extracts unraveled the presence of 44 metabolites in EAE and 39 metabolites in CSE, mostly described for the first time in EAE and CSE. In this sense, Figure 2A,B exhibits the base peak chromatograms (BPCs) of EAE (A) and CSE (B) in both negative and positive ionization modes, whereas Figure 2C,D demonstrates the bubble plots of the annotated metabolite masses (m/z) vs the retention time (RT) considering metabolite classes. The observed metabolites were grouped and classified into phenolic derivatives (5), nitrogenous compounds (22), fatty acids and rhamnolipids (4), lactones, furans, and organic acids (7), and terpenes and sterols (6). In brief, the molecular ion peaks (m/z), retention times (RTs),

Table 1. Metabolites Characterized in *E. asperum* and *C. siphonella*^a

Peak no.	RT (min)	[M-H] ⁺	[M+H] ⁺	Molecular formula	Score	Error (mDa)	Main fragments	DBE	Proposed compound	Class	Species	Reference	<i>Echinodictyum asperum</i>	%	<i>Callyspongia siphonella</i>	%
1	0.75		148.0965	C ₆ H ₁₃ NO ₃	98.98	0.39	131.0878, 130.0853	1	Hydroxyleucine/Hydroxyisoleucine	Am	<i>Theonella swinhoei</i>	²³	3.28E+07	3.92	0.00E+00	0.00
2	0.75		194.1017	C ₇ H ₁₅ NO ₅	88.54	0.08		1	N-methyl-D-glucosamine I	Am	<i>Halichondria cylindrata</i>	²³	1.57E+07	1.88	0.00E+00	0.00
3	0.77		118.0870	C ₅ H ₁₁ NO ₂	82.32	-0.68	101.0231, 100.0768	1	Valine I	Am	<i>Arthrospira platensis</i>	³	5.32E+07	6.36	5.26E+06	0.70
4	0.87		162.1118	C ₇ H ₁₅ NO ₃	82.54	0.77	145.0105, 101.0155	1	Carnitin	Am	<i>Callyspongia sp.</i>	²³	7.24E+06	0.87	7.73E+06	1.02
5	0.99		132.1013	C ₆ H ₁₃ NO ₂	96.92	0.67	114.9498	1	Leucine/Isoleucine I	Am	<i>Arthrospira platensis</i>	³	7.54E+06	0.90	7.62E+06	1.01
6	0.99	365.1373	367.1504	C ₁₇ H ₂₂ N ₂ O ₇	97.89	-0.59	N.D.	8	Mannosyl tryptophan I	Am	<i>Leptoclinides dubius</i>	²³	3.15E+06	0.38	0.00E+00	0.00
7	1.23		146.1164	C ₇ H ₁₅ NO ₂	79.37	1.04	N.D.	1	Leucine methyl ester	Am	<i>Aspergillus sp</i>	²³	6.91E+06	0.83	1.37E+06	0.18
8	1.34		367.1503	C ₁₇ H ₂₂ N ₂ O ₇	78.68	0.80	205.0842	8	Mannosyl tryptophan II	Am	<i>Leptoclinides dubius</i>	²³	2.29E+06	0.27	0.00E+00	0.00
9	2.04		118.0870	C ₅ H ₁₁ NO ₂	87.21	0.03	N.D.	1	Valine II	Am	<i>Arthrospira platensis</i>	³	9.82E+06	1.17	0.00E+00	0.00
10	2.16		194.1016	C ₇ H ₁₅ NO ₅	96.99	0.68		1	N-methyl-D-glucosamine II	Am	<i>Halichondria cylindrata</i>	²³	6.02E+06	0.72	0.00E+00	0.00
11	2.58		132.1032	C ₆ H ₁₃ NO ₂	72.77	-0.76	N.D.	1	Leucine/Isoleucine II	Am	<i>Arthrospira platensis</i>	³	1.39E+06	0.17	1.48E+06	0.20
12	15.64	345.1567		C ₁₆ H ₂₈ O ₈	84.63	-2.15	217.1047, 127.0411	4	3-O-butylglyceryl-2-O-allyl ascorbic acid	O		²³	5.58E+05	0.07	6.85E+05	0.09
13	21.88		369.1543	C ₁₈ H ₂₄ O ₈	97.67	0.20	300.0969, 258.0442,	7	Hyptolide	L	<i>Hyptis pectinata</i>	²³	1.40E+07	1.68	1.65E+07	2.18
14	23.52		205.0600	C ₁₀ H ₈ N ₂ O ₃	61.09	0.88	N.D.	8	Hemimycalin C	A	<i>Hemimycala sp.</i>	¹³	4.15E+05	0.05	7.79E+05	0.10
15	23.52		513.1966	C ₂₄ H ₃₂ O ₁₂	95.00	0.13	N.D.	9	6-O-(3,4-dimethoxybenzoyl)-ajugol	I	<i>Tabebuia avellanedae</i>	²³	5.14E+06	0.61	5.79E+06	0.77
16	26.05		541.2265	C ₂₆ H ₃₆ O ₁₂	97.60	-13	N.D.	9	Briarenon H/J / Briarexavatin L/S	B	<i>Briareum excavatum</i>	¹³	8.80E+06	1.05	7.76E+06	1.03
17	27.15		325.2374	C ₁₉ H ₃₂ O ₄	99.87	-0.04	307.2282, 289.2137, 165.1300	4	8aH,9aH-11,12-diacetoxymirane	D	<i>Dysidea fusca</i>	¹³	9.55E+06	1.14	1.40E+07	1.86
18	27.28		307.2283	C ₁₉ H ₃₀ O ₃	88.36	-1.42	N.D.	5	6-desmethyl-6-ethylspongisoritin A I	F	<i>Plakortis sp.</i>	¹³	1.83E+06	0.22	2.36E+06	0.31
19	27.63		307.2285	C ₁₉ H ₃₀ O ₃	89.41	-1.80	N.D.	5	6-desmethyl-6-ethylspongisoritin A II	F	<i>Plakortis sp.</i>	¹³	7.49E+06	0.89	1.54E+07	2.04
20	27.85		309.2420	C ₁₉ H ₃₂ O ₃	94.62	0.73	291.2281, 228.9971	4	Methyl (2Z,6R,8S)-4,6-diethyl-3,6-epoxy-8-methyldeca-2,4-dienoate I	F	<i>Plakortis sp.</i>	¹³	2.98E+06	0.36	3.17E+06	0.42
21	28.20		323.2219	C ₁₉ H ₃₀ O ₄	93.64	-0.30	N.D.	5	Plakorfuran A	F	<i>Plakortis simplex</i>	¹³	4.01E+06	0.48	2.82E+06	0.37
22	31.25	353.2151	355.2266	C ₂₃ H ₃₀ O ₃	98.83	0.05	337.2851, 293.1003, 275.1772	9	15/18β-acetoxypregna-1,4,20-trien-3-one I	P	<i>Carijoa sp.</i>	¹³	2.90E+06	0.35	2.49E+06	0.33
23	33.71		256.2635	C ₁₆ H ₃₃ NO	98.33	0.17	N.D.	1	Palmitamide I	La	<i>CEAetoceros sp.</i>	²³	1.11E+07	1.32	1.13E+07	1.50
24	34.06		309.2420	C ₁₉ H ₃₂ O ₃	97.45	-0.41	N.D.	4	Methyl (2Z,6R,8S)-4,6-diethyl-3,6-epoxy-8-methyldeca-2,4-dienoate II	F	<i>Plakortis sp.</i>	¹³	8.16E+07	9.75	8.49E+07	11.26
25	34.08		256.2646	C ₁₆ H ₃₃ NO	95.84	-0.90	N.D.	1	Palmitamide II	La	<i>CEAetoceros sp.</i>	²³	4.93E+06	0.59	6.38E+06	0.85
26	34.19		331.2266	C ₂₁ H ₃₀ O ₃	97.25	0.21	267.1729	7	Cladosporisteroid B	S	<i>Cladosporium sp.</i>	¹³	2.07E+06	0.25	1.75E+06	0.23

Table 1. continued

Peak no.	RT (min)	[M-H] ⁺	[M+H] ⁺	Molecular formula	Score	Error (mDa)	Main fragments	DBE	Proposed compound	Class	Species	Reference	<i>Echinodictyum asperum</i>	%	<i>Calyspongia siphonella</i>	%
27	34.41	339.2352		C ₂₃ H ₃₂ O ₂	86.38	-2.18	163.1132	8	2,2'-Bis(4-methyl-6-tert-butylphenol) methane I	Ph	<i>Arthrospira platensis</i>	³	5.45E+07	6.51	5.33E+07	7.07
28	34.65		270.2797	C ₁₇ H ₃₅ NO	95.47	0.32	235.2365, 224.8165, 100.1134	1	Bacillamadin G	La	<i>Bacillus pumilus</i>	¹³	8.98E+06	1.07	1.16E+07	1.54
29	35.01	453.2280		C ₂₇ H ₃₄ O ₆	93.03	0.04	N.D.	11	Chromequinoline I	Q	<i>Arthrospira platensis</i>	³	1.97E+06	0.24	3.11E+06	0.41
30	35.01	423.2931		C ₂₈ H ₄₀ O ₃	85.66	-2.54	N.D.	9	Tetraprenylhydroquinone derivative	Q	<i>Ircinia muscarum</i>	¹³	4.31E+05	0.05	0.00E+00	0.00
31	35.12	279.2343	281.2492	C ₁₈ H ₃₂ O ₂	81.71	-1.63	N.D.	3	Linoleic acid	Fa	<i>Arthrospira platensis</i>	³	9.27E+06	1.11	9.45E+06	1.25
32	35.70		284.2945	C ₁₈ H ₃₇ NO	98.68	0.36	N.D.	1	N-isopentyltridecanamide I	La	<i>Streptomyces sp.</i>	¹³	6.77E+06	0.81	7.95E+06	1.05
33	36.88	255.2343	257.2477	C ₁₆ H ₃₂ O ₂	92.89	-1.35	236.9891	1	Palmitic acid	Fa	<i>Arthrospira platensis</i>	³	9.74E+06	1.16	8.29E+06	1.10
34	36.99		284.2945	C ₁₈ H ₃₇ NO	99.24	0.26	N.D.	1	N-isopentyltridecanamide II	La	<i>Streptomyces sp.</i>	¹³	1.27E+07	1.52	1.30E+07	1.73
35	36.99	459.2944		C ₂₄ H ₄₄ O ₈	85.59	1.98	N.D.	3	Dokdolipid B	Rh	<i>Actinoalloteichus hymeniacidonis</i>	¹³	2.02E+06	0.24	3.52E+06	0.47
36	37.46		284.2945	C ₁₈ H ₃₇ NO	97.00	0.41	N.D.	1	N-isopentyltridecanamide III	La	<i>Streptomyces sp.</i>	¹³	2.25E+08	26.87	2.30E+08	30.53
37	37.83		310.3121	C ₂₀ H ₃₉ NO	74.74	1.77	N.D.	2	Cis-11-eicosenamide I	La	<i>Alcanivorax sp.</i>	²³	1.71E+07	2.05	2.04E+07	2.70
38	38.18		310.3119	C ₂₀ H ₃₉ NO	79.04	-1.46	N.D.	2	Cis-11-eicosenamide II	La	<i>Alcanivorax sp.</i>	²³	6.42E+06	0.77	9.54E+06	1.27
39	38.40		310.3102	C ₂₀ H ₃₉ NO	85.19	0.23	N.D.	2	Cis-11-eicosenamide III	La	<i>Alcanivorax sp.</i>	²³	3.40E+07	4.07	3.51E+07	4.66
40	39.47	283.2659		C ₁₈ H ₃₆ O ₂	90.1	-1.71	262.6257	1	Stearic acid	Fa	<i>Arthrospira platensis</i>	³	4.22E+05	0.05	2.30E+05	0.03
41	40.28		312.3254	C ₂₀ H ₄₁ NO	96.2	0.71	N.D.	1	Eicosanamide	La	<i>Paederia foetida</i>	²³	1.41E+08	16.82	1.46E+08	19.41
42	43.81	339.2347		C ₂₃ H ₃₂ O ₂	89.46	-1.85	N.D.	8	2,2'-Bis(4-methyl-6-tert-butylphenol) methane II	Ph	<i>Arthrospira platensis</i>	³	2.40E+06	0.29	1.76E+06	0.23
43	43.91	353.2138	355.2266	C ₂₃ H ₃₀ O ₃	90.35	-1.62	N.D.	9	15/18β-acetoxypregna-1,4,20-trien-3-one II	P	<i>Carijoa sp.</i>	¹³	5.69E+05	0.07	4.75E+05	0.06
44	44.04	453.2282		C ₂₇ H ₃₄ O ₆	97.16	-0.18	N.D.	11	Chromequinoline II	Q	<i>Arthrospira platensis</i>	³	4.18E+05	0.05	2.36E+05	0.03

^aA; Alkaloids, Am; Amino acids, B; Briarane-type diterpenoids, D; Drimane sesquiterpenes, F; Furans, Fa; Fatty acids, I; Iridoid glycosides, O; Organic acids, L; lactones, La; Long-chain amides, P; Pregnanes, Ph; Phenols, Q; Quinones, Rh; Rhamnolipids, S; Sterols, DBE, Double bond equivalence, N.D., undetected. Peak area: lowest value  highest value.

neutral losses, generated molecular formulas, double bond equivalence (DBE), and relative abundance (peak area of each metabolite) were observed and compared with the relevant literature^{24,33} (Figure 2 and Table 1).

In this context, the characterized nitrogenous compounds were the most abundant, accounting for 22 metabolites qualitatively and a relative abundance of 73.39 and 68.44% quantitatively for EAE and CSE, respectively.

They were subclassified into alkaloids (1), long-chain amides (10), and amino acids (11). Alkaloid hemimycalin C was detected in both EAE and CSE. Also, long-chain amides were mentioned for the first time in both EAE and CSE, which are the

major metabolites in terms of relative abundance. They are palmitidine I–II, bacillamadin G, N-isopentyltridecanamide I–III, cis-11-eicosenamide I–III, and eicosanamide (Table 1). Moreover, 11 amino acids were noticed: valine I–II and leucine/isoleucine I–II alongside their methoxylated and acetylated derivatives alongside carnitine. Besides, N-methyl-D-glucosamine I–II and mannosyl tryptophan I–II were noticed to be present in EAE only. It is worth noting that the characterized amino acids were noticed for the first time in EAE and CSE and their characterization as per previous studies³⁴ (Table 1, Figures 3, and 4).

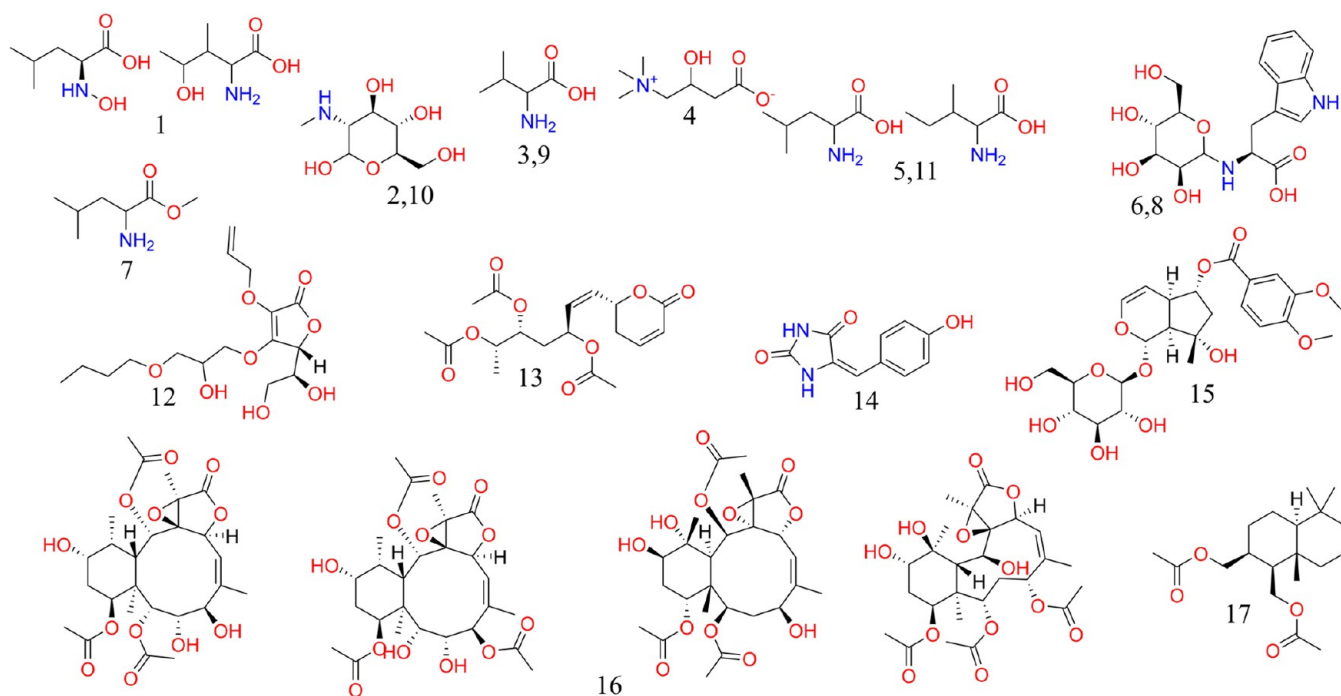


Figure 3. Chemical structures of the metabolites characterized in *E. asperum* and *C. siphonella* (compounds 1–17).

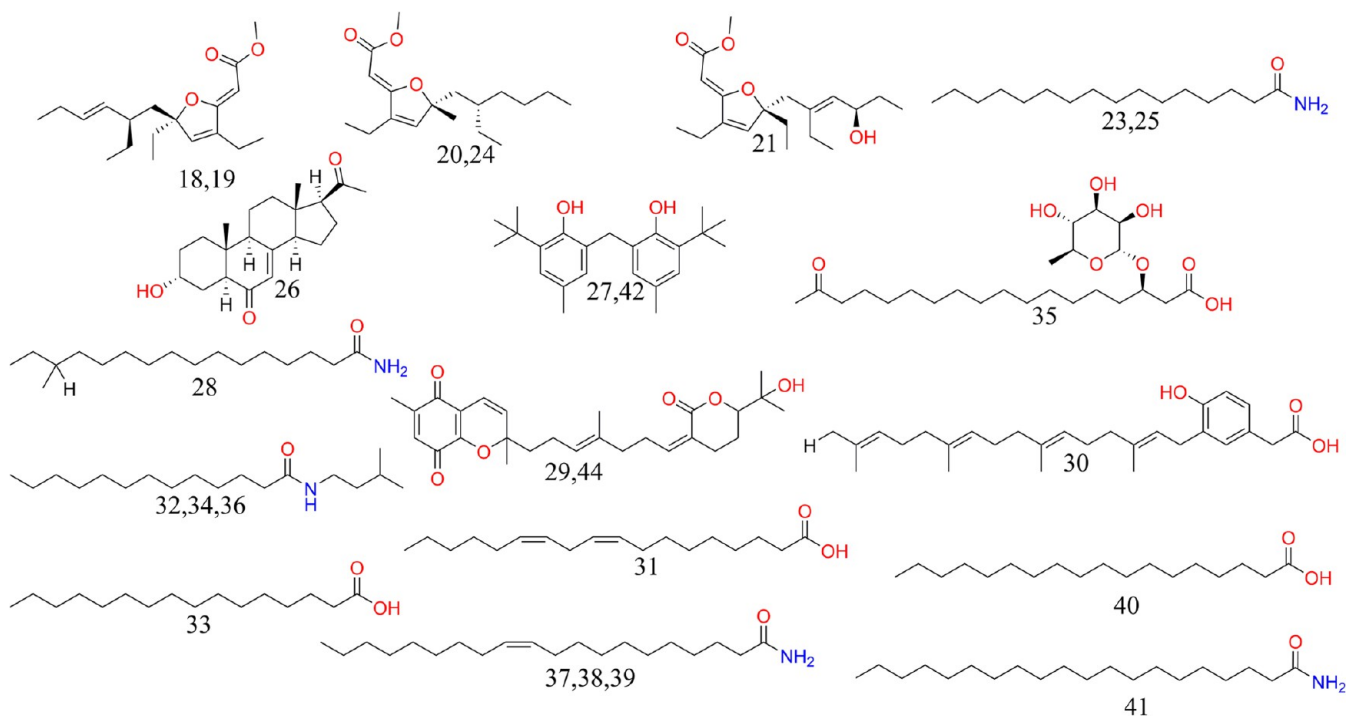


Figure 4. Chemical structures of the metabolites characterized in *E. asperum* and *C. siphonella* (compounds 18–44).

Phenolic derivatives were represented by two isomers of chromequinolide I–II ($C_{27}H_{34}O_6$, m/z 453.23), 2,2'-bis(4-methyl-6-*tert*-butylphenol) methane I–II ($C_{23}H_{32}O_2$, m/z 339.23),³ and a tetraprenylhydroquinone derivative ($C_{28}H_{40}O_3$, m/z 423.29), which was present in EAE only.¹³ It is worth mentioning that phenolic derivatives accounted for 7.1 and 7.8% of the relative abundances of EAE and CSE, respectively.

Four fatty acids and rhamnolipids were observed where their characterization agrees with.^{3,13,23} In this context, it is worth

noting that dokdolipid B ($C_{24}H_{44}O_8$, m/z 459.2944) was recognized in CSE and EAE as a representative of rhamnolipids. In contrast, long-chain saturated fatty acids were noticed, *viz.*, palmitic acid (C16:0) and stearic acid (C18:0). Moreover, linoleic acid (C18:2) was characterized as an example of long-chain diunsaturated fatty acids (Table 1, Figures 3, and 4).

With regard to terpenoids and sterols, three terpenoid derivatives were observed in EAE and CSE. In this line, 8*α*H,9*α*H-11,12-diacetoxymethane ($C_{19}H_{32}O_4$, m/z 325.24) was noticed as an example of drimane sesquiterpene.¹³ As for

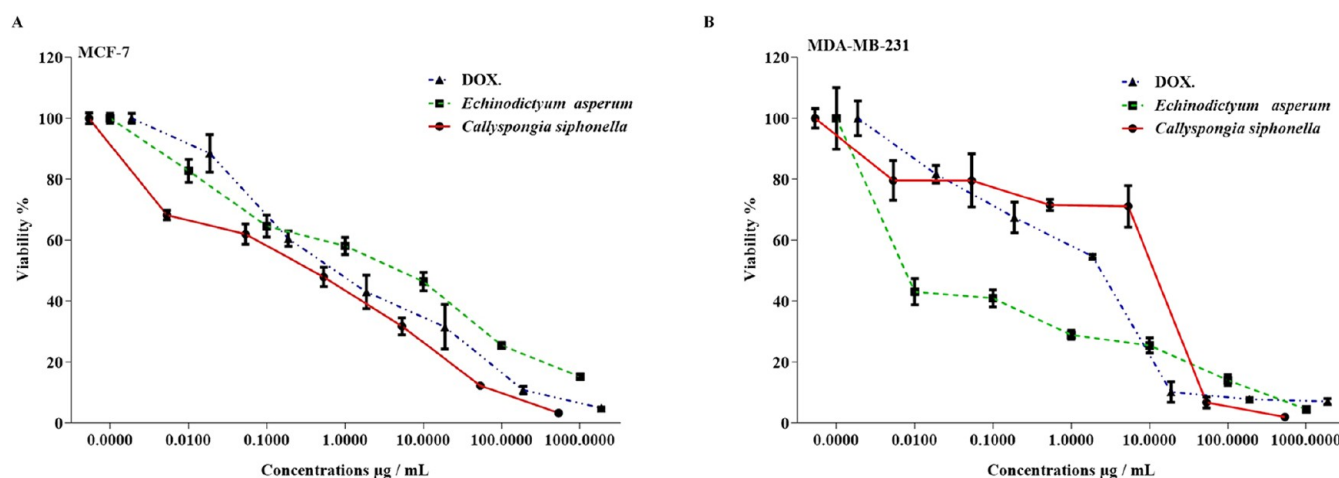


Figure 5. Cytotoxic effect of *E. asperum* (EAE) and *C. siphonella* (CSE) on (A) MCF-7 and (B) MDA-MB-231 cell lines. The IC₅₀ value corresponds to the concentration leading to a loss of 50% of cell viability. Data are presented as mean values \pm standard error of the mean (SEM) based on three replicates ($n = 3$).

iridoid glycosides, 6-*O*-(3,4-dimethoxybenzoyl)-ajugol ($\text{C}_{24}\text{H}_{32}\text{O}_{12}$, m/z 513.20) was present.²³ Also, a briarane-type diterpenoid was detected where the ion of the m/z 514.23 and molecular formula $\text{C}_{26}\text{H}_{36}\text{O}_{12}$ were characterized as briarenol H/J/briaexcavatin L/S (Table 1 and Figure 3).¹³ Moreover, three sterols were noticed in EAE and CSE, *viz.*, cladosporisteroid B ($\text{C}_{21}\text{H}_{30}\text{O}_3$, m/z 331.23) and 15/18 β -acetoxypregna-1,4,20-trien-3-one I–II as examples of pregame sterols.

With respect to lactones, furans, and organic acids, seven derivatives were characterized in EAE and CSE, constituting 13.44 and 16.68% of the relative abundances of EAE and CSE, respectively. In this regard, organic acids and lactones were represented by 3-*O*-butylglyceryl-2-*O*-allyl ascorbic acid ($\text{C}_{16}\text{H}_{28}\text{O}_8$, m/z 345.16) and hyptolide ($\text{C}_{18}\text{H}_{24}\text{O}_8$, m/z 369.1) in a respective manner.²³ Furthermore, four furan derivatives were annotated and described before in the genus of marine sponges, *Plakortis*. They were described as 6-desmethyl-6-ethylspongisoritin I–II, methyl (2*Z*,6*R*,8*S*)-4,6-diethyl-3,6-epoxy-8-methyldeca-2,4-dienoate I–II, and plakorfuran (Table 1, Figures 3, and 4).

3.2. Cell Viability Assay. The cytotoxic effects of EAE and CSE on human breast cancer were assessed by exposing MCF-7 and MDA-MB-231 cells to different concentrations of the extracts (ranging from 0.01 to 1000 $\mu\text{g/mL}$) for a duration of 72 h. The half-maximal inhibitory concentration (IC₅₀) after 72 h of exposure was determined using the sulforhodamine B (SRB) reduction assay to measure cell viability. The IC₅₀ value for *E. asperum* extract (EAE) was approximately 0.5 $\mu\text{g/mL}$ for MCF-7 cells, while for *C. siphonella* (CSE), it was around 2.7 $\mu\text{g/mL}$ (Figure 5A). Similarly, for MDA-MB-231 cells, the IC₅₀ value for EAE was approximately 8.7 $\mu\text{g/mL}$, whereas for CSE, it was around 45.3 $\mu\text{g/mL}$ (Figure 5B). These findings indicate the concentration at which each extract inhibits cell growth by 50%, providing valuable insights into its cytotoxic potential against breast cancer cells.

3.3. Apoptosis. To identify the form of cell death induced by EAE and CSE, the tested cancer cell lines were incubated for 48 h with the various antitumor molecules at IC₅₀. Cells were then analyzed using the Annexin/V-FITC, and subsequently, apoptotic and necrotic cells were differentiated by flow cytometry apoptosis detection assay.

In MCF-7 cells (Figure 6), the double-stained (Annexin V +/PI+) cells were increased from 0.97% (the control group) to 59.92% after the treatment of EAE at 0.5 $\mu\text{g/mL}$ and to 70.72% after the treatment of CSE at 2.7 $\mu\text{g/mL}$ in a dose-dependent manner. The percentage of (Annexin V+/PI+) in MDA-MB-231 cells was increased from 0.47% in the control group to 70.84% after the treatment of EAE at 8.7 $\mu\text{g/mL}$ and to 59.58% after the treatment of CSE at 45.3 $\mu\text{g/mL}$ in a dose-dependent manner (Figure 7). It is notable that the necrotic cells were increased after treatment with sponges' extract (5.03 and 9.95%, respectively) compared with the control group (0.24%) in MCF-7 cells and (5.16 and 14.34%, respectively) compared to the control group (0.17%) in MDA-MB-231 cells, which suggested that treatment with sponges' extracts seemed to accelerate cell death by necrosis and late apoptosis.

3.4. Cell Cycle Analysis. To investigate the potential antiproliferative effects of EAE and CSE against cancer cells, the MCF-7 and MDA-MB-231 cell lines were incubated for 48 h with sponges' extracts at IC₅₀ values. This will determine whether the antiproliferative effect was due to the arrest of the cell cycle at a specific phase. Cell cycle arrest in the growth phase by antitumor molecules leads to cell death by apoptosis. Damaged cells undergo apoptosis through cell cycle arrest into the G1 or G2 phases, usually due to subsequent aberrant mitosis. This usually occurs as late apoptosis resulting from several distinct pathways, such as DNA damage, resulting in cell arrest in the G1 or G2/M phase. Subsequently, the cell cycle phases were analyzed using DNA content flow cytometry (Figure 8). EAE exerted an antiproliferative effect and arrested the cell cycle of the MCF-7 cell lines in the G2 phase (Figure 8), while the CSE significantly increased the cell population at the S phase (Figure 8). In response to the EAE and CSE in MDA-MB-231 cell lines, the cell population in the S phase significantly increased (Figure 9), indicating a robust antiproliferative effect as compared to nontreated cells.

3.5. Autophagy. Autophagy is a lysosomal degradation process that targets cytoplasmic constituents, particularly under stress conditions. To investigate whether sponge extracts (EAE) and (CSE) could induce autophagy in breast cancer cells, we performed experiments using acridine orange staining to detect autophagic cells. In MCF-7 cells treated with 0.5 $\mu\text{g/mL}$ of EAE and 2.7 $\mu\text{g/mL}$ of CSE (Figure 10), there was no significant

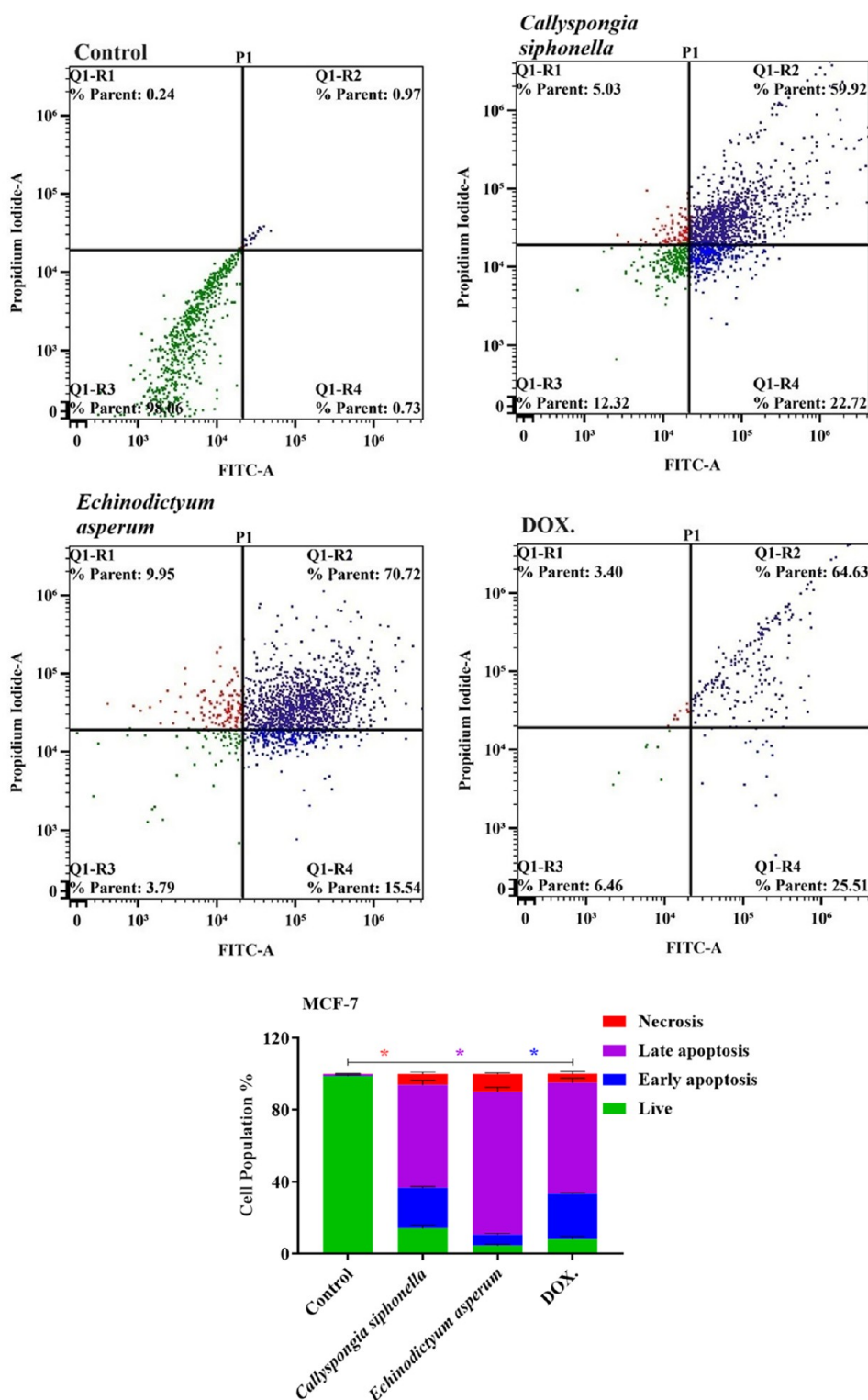


Figure 6. Cell populations in different stages (live, apoptotic, and necrotic) following the extract treatment (EAE) and (CSE) of MCF-7 cells for 48 h and evaluated by double staining in Annexin V-FITC/propidium iodide using a flow cytometric assay. The data are presented as mean values \pm SD based on three replicates ($n = 3$). Significance was determined by comparing the events from each respective control, with differences considered significant at * $p > 0.05$; ** $p < 0.01$; and *** $p < 0.001$.

change in the percentage of autophagic cells. In contrast, treatment with the extracts in MDA-MB-231 cells resulted in a notable increase in the level of formation of autophagic cells (Figure 11). This suggests a cell-line-specific response to the sponge extracts, with MDA-MB-231 cells showing a heightened autophagic response.

3.6. Molecular Docking. The binding free energies of the major constituents from (EAE) and (CSE) extracts were evaluated against the targets BCL-2, MCL-1, and ER α , compared to the cocrystallized ligands and the positive control, doxorubicin (Table 2). The cocrystallized ligands showed the best docking scores for all three targets, with values of -9.75

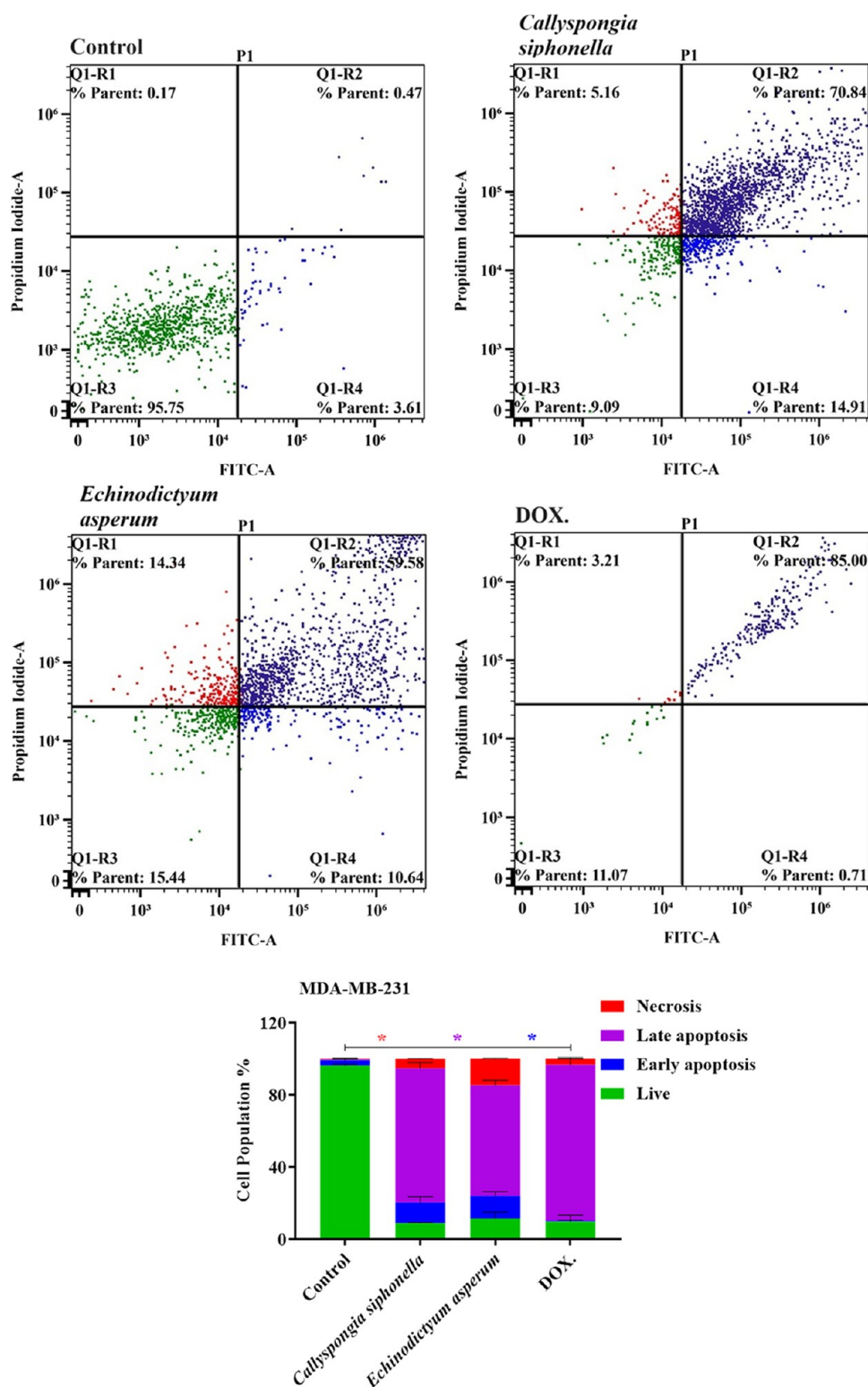


Figure 7. Cell populations in different stages (live, apoptotic, and necrotic) following the extract treatment (EAE) and (CSE) of MDA-MB-231 cells for 48 h and evaluated by double staining in Annexin V-FITC/propidium iodide using a flow cytometric assay. The data are presented as mean values \pm SD based on three replicates ($n = 3$). Significance was determined by comparing the events from each respective control, with differences considered significant at * $p > 0.05$; ** $p < 0.01$; and *** $p < 0.001$.

kcal/mol for BCL-2, -8.66 kcal/mol for MCL-1, and -9.16 kcal/mol for ER α . Among the extracts, cis-11-nicotinamide I–III, hyptolide, palmitamide I–II, bacillamadin G, and *N*-isopentyltridecanamide I–III demonstrated competitive binding affinities, especially hyptolide, which exhibited a strong

docking score of -9.17 kcal/mol for ER α , outperforming doxorubicin's score of 5.15 kcal/mol for this target.

The redocking of ABT-199 resulted in a very high binding affinity (-9.75 kcal/mol) and an root mean square deviation (RMSD) value of 0.67 , which confirms the validity of the

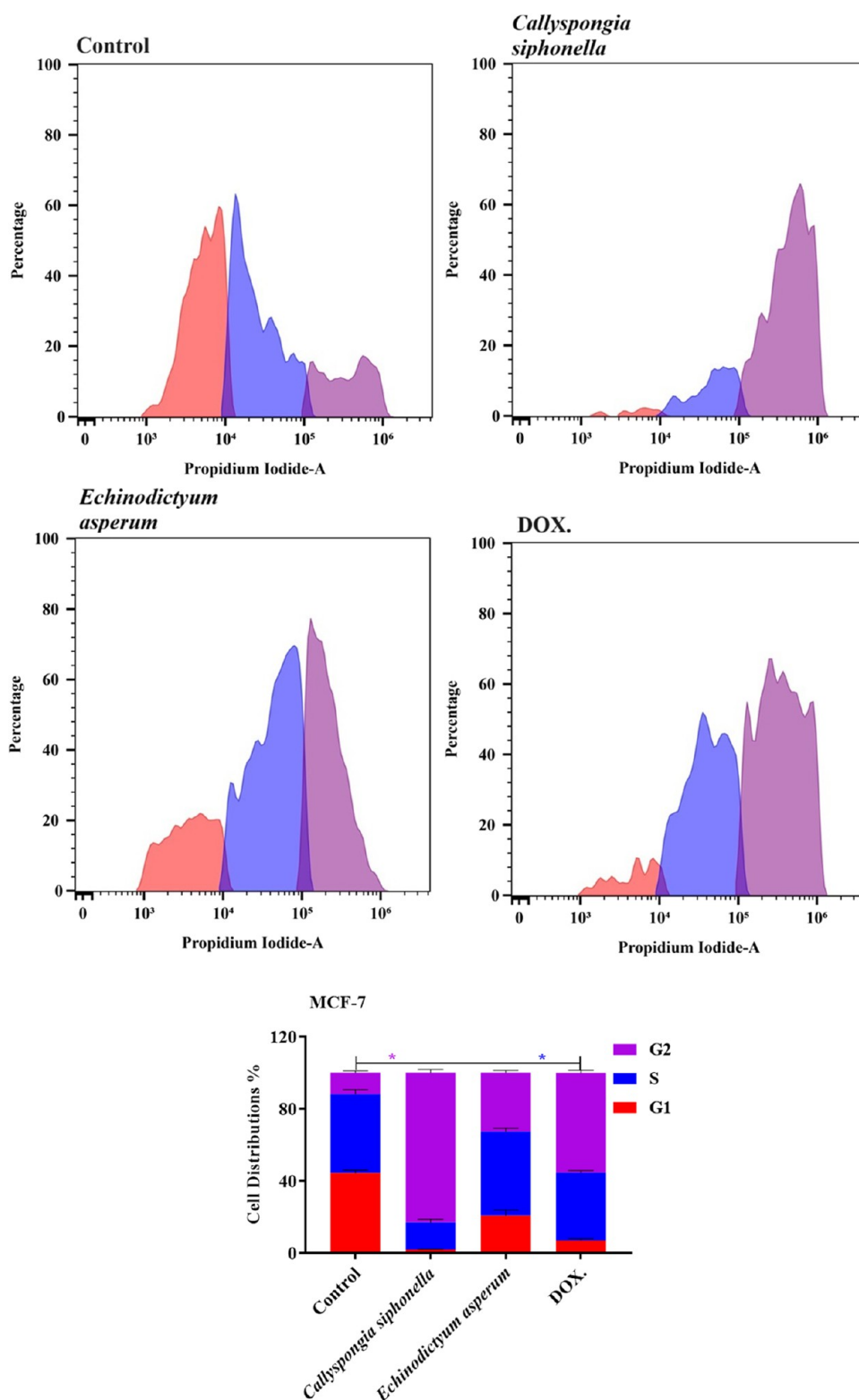


Figure 8. DNA content distribution of cell cycle phases of MCF-7 cells treated with precalculated IC₅₀ of (EAE) and (CSE) for 48 h represents cell control. The data are presented as mean values \pm SD based on three replicates ($n = 3$). Significance was determined by comparing the events from each respective control, with differences considered significant at * $p > 0.05$; ** $p < 0.01$; and *** $p < 0.001$.

docking protocol. ABT-199 bound to BCL-2 through a series of strong interactions, including four hydrogen bonds (H-bonds) with Asp100, Asn140, Gly142, and Tyr199, four ionic interactions with Asp100 and Asp108, an ion- π interaction with Asp108, and π - π stacking with Tyr105 (Figure 12A).

These interactions suggest a highly stable binding mode for ABT-199, as reflected in its superior binding affinity (Table 2).

Doxorubicin, used as a positive control, also demonstrated good binding to BCL-2, with a binding affinity of -7.27 kcal/mol. Doxorubicin formed 4 H-bonds with Asp108, Asp137,

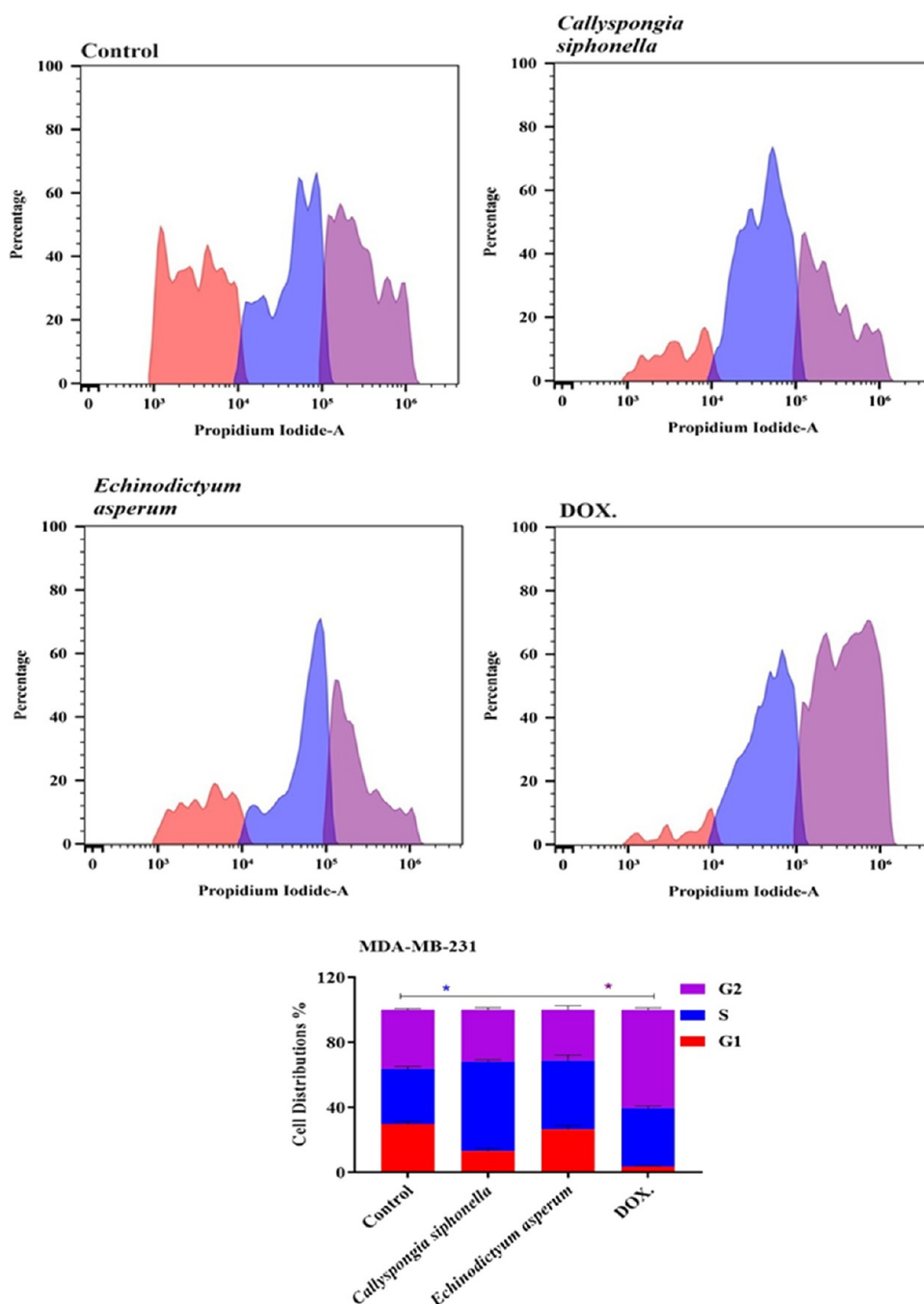


Figure 9. DNA content distribution of cell cycle phases of MDA-MB-231 cells treated with precalculated IC_{50} of (EAE) and (CSE) for 48 h represents cell control. The data are presented as mean values \pm SD based on three replicates ($n = 3$). Significance was determined by comparing the events from each respective control, with differences considered significant at * $p > 0.05$; ** $p < 0.01$; and *** $p < 0.001$.

Asn140, and Arg143, as well as 3 ionic interactions with Asp108, Arg143, and Glu133 (Figure 12B).

Among the constituents of (EAE) and (CSE), cis-11-eicosenamide I–III, which is present in both extracts in significant amounts (6.88 and 8.63%, respectively), exhibited the highest binding affinity (−7.02 kcal/mol), which is slightly lower than that of doxorubicin (−7.27 kcal/mol) (Table 1). Cis-11-eicosenamide formed only one H-bond with Asp100, alongside several hydrophobic interactions due to its long aliphatic chain (Figure 10G). The presence of this H-bond with Asp100, a key residue in the active site of BCL-2, is likely responsible for the relatively strong binding affinity of this

compound, although the absence of additional H-bonds or ionic interactions limits its binding strength.

Eicosanamide, another major constituent, exhibited a binding affinity similar to that of cis-11-eicosenamide (−6.98 kcal/mol) (Table 1). Eicosanamide binding mode relied entirely on hydrophobic interactions between its aliphatic chain and the hydrophobic residues in the BCL-2 pocket, including Tyr105, a residue also involved in the binding of ABT-199 (Figure 12D). The lack of H-bonding or ionic interactions with key residues like Asp100 or Asp108 may explain the slightly reduced affinity of eicosanamide compared to that of cis-11-eicosenamide.

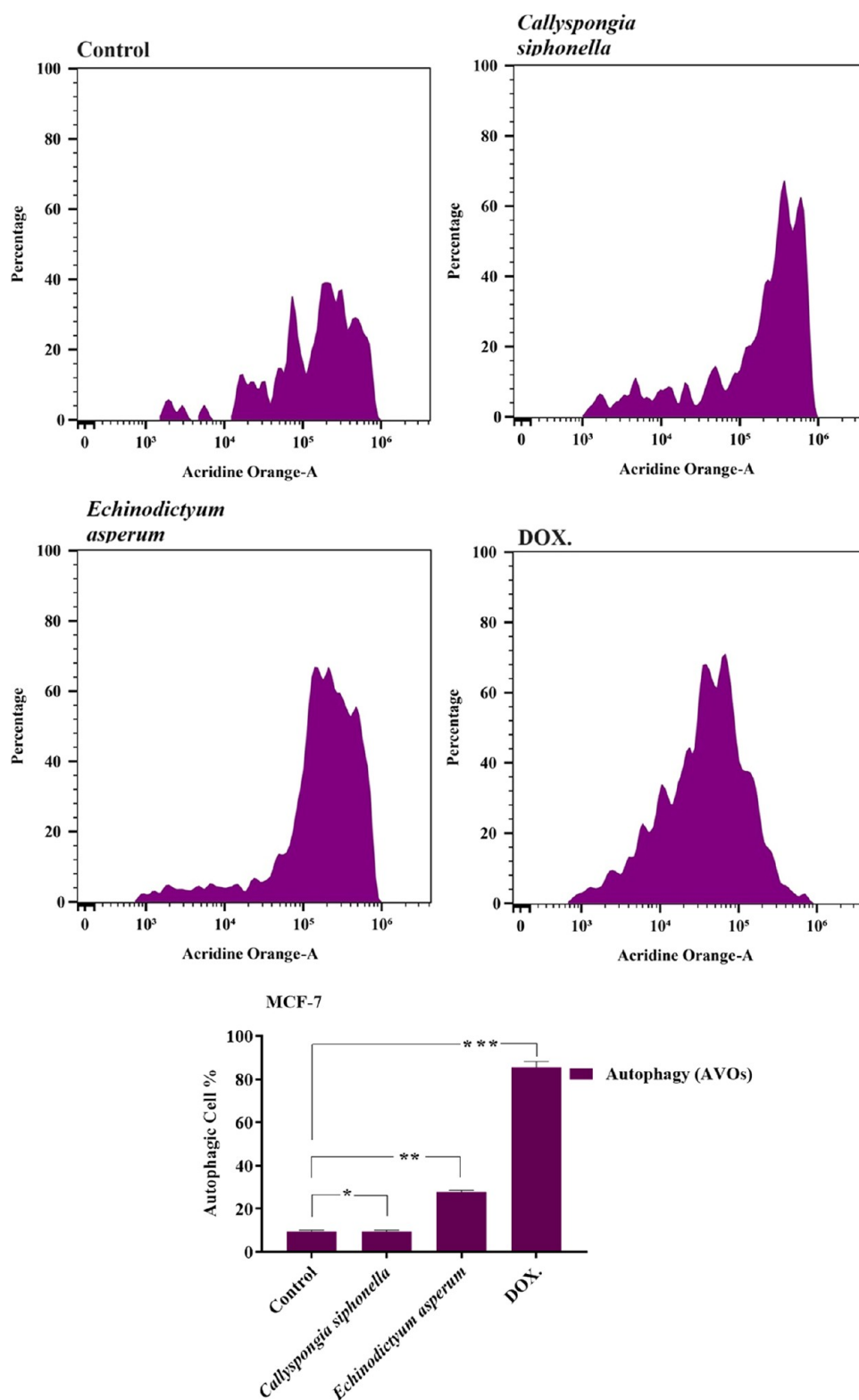


Figure 10. Effects of sponge extracts EAE and CSE on autophagy in MCF-7 cells. Acidic vesicular organelles were detected and quantified using acridine orange staining and measured using flow cytometry analysis. Acridine orange ($1 \mu\text{g/mL}$) staining was used to identify autophagic cells via FACS. The data are presented as mean values \pm SD based on three replicates ($n = 3$). Significance was determined by comparing the events from each respective control, with differences considered significant at * $p > 0.05$; ** $p < 0.01$; and *** $p < 0.001$.

N-Isopentyltridecanamide I–III, the most abundant component in both extracts, showed a binding affinity of -6.20 kcal/mol (Table 1). It formed similar interactions to *cis*-11-eicosenamide, with one H-bond and several hydrophobic

interactions, possibly due to the similarity in their chemical structures (Figure 12C). The weaker binding affinity of *N*-isopentyltridecanamide compared with that of *cis*-11-eicosena-

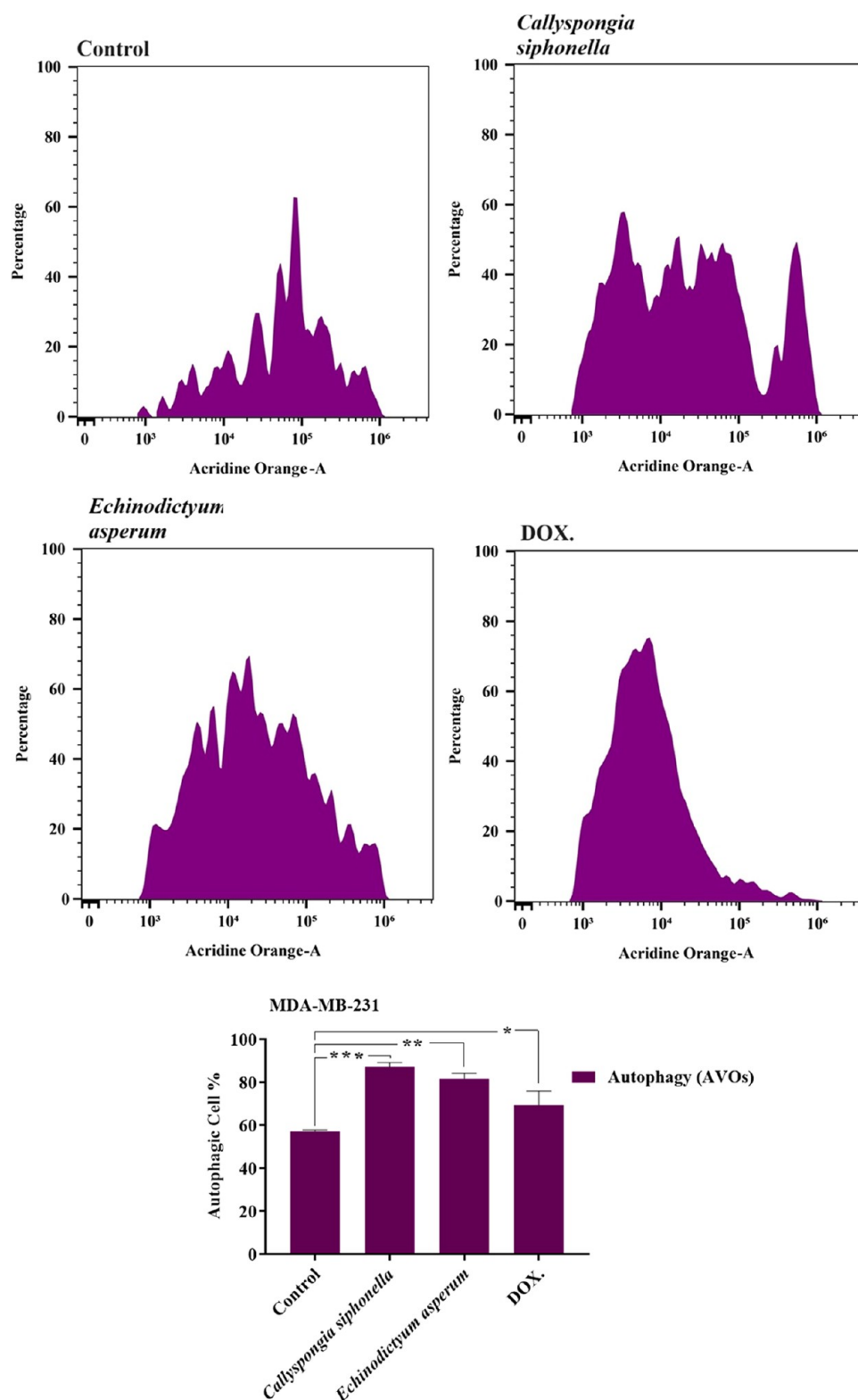


Figure 11. Effects of sponge extracts EAE and CSE on autophagy in MDA-MB-231 cells. Acidic vesicular organelles were detected and quantified using acridine orange staining and measured using flow cytometry analysis. Acridine orange (1 $\mu\text{g/mL}$) staining was used to identify autophagic cells via FACS. The data are presented as mean values \pm SD based on three replicates ($n = 3$). Significance was determined by comparing the events from each respective control, with differences considered significant at * $p > 0.05$; ** $p < 0.01$; and *** $p < 0.001$.

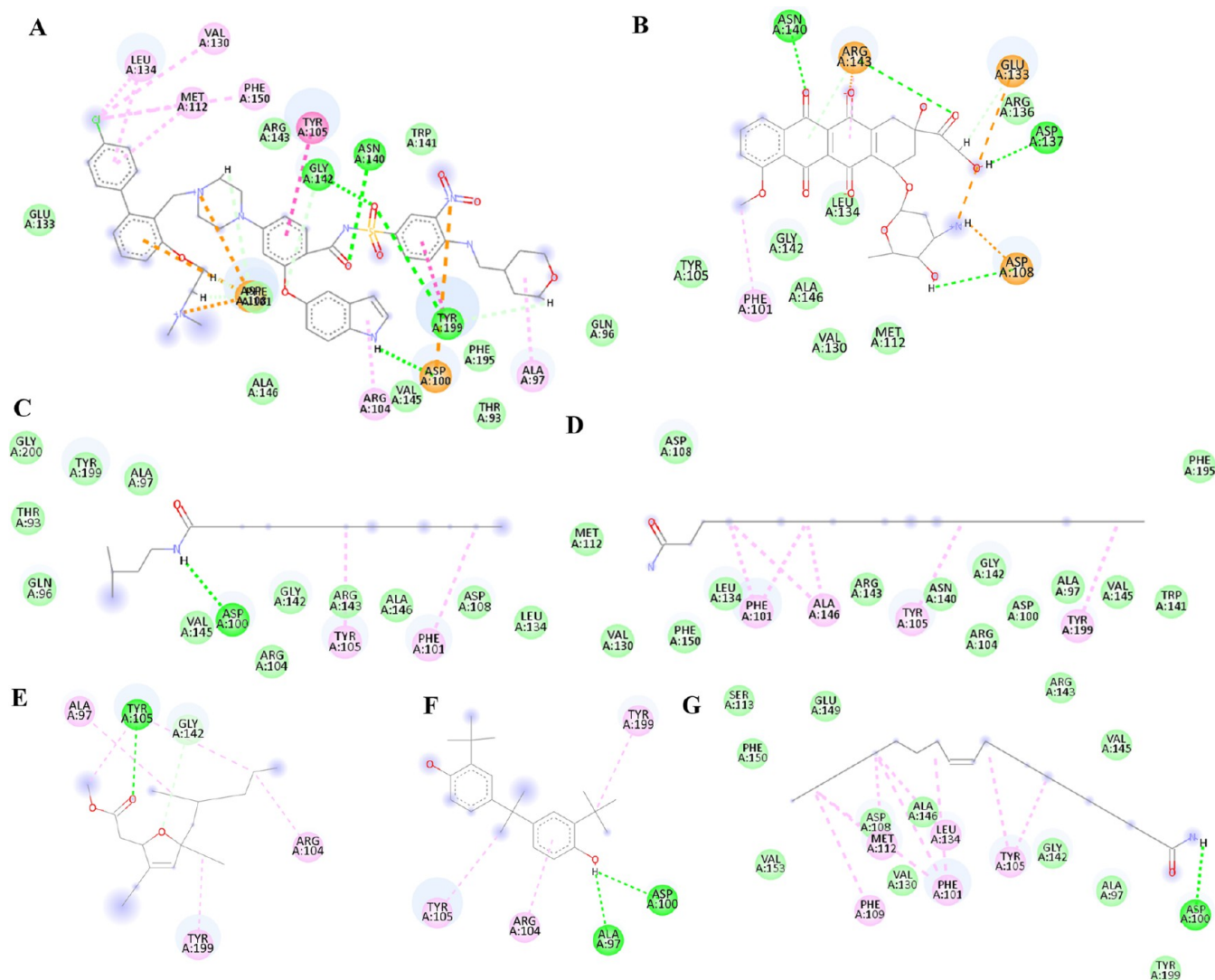
vide suggests that subtle structural differences may influence its interaction with BCL-2.

Hyptolide exhibited a binding affinity of -6.13 kcal/mol and formed 3 H-bonds with Asn140, Gly142, and Tyr199, residues

that are also involved in the binding of ABT-199 (Figure 13C). The presence of multiple carbonyl groups in hyptolide likely contributed to these H-bonds, enhancing its binding affinity. Despite these similarities, the hyptolide binding affinity was

Table 2. Free Energies of Binding for (EAE) and (CSE) Major Extracts' Constituents against BCL-2, MCL-1, and ER α Compared to Their Cocrystallized Ligands and Positive Control (Doxorubicin)

compound	docking score ΔG (kcal/mol)		
	BCL-2	MCL-1	ER α
cocrystallized ligand	−9.75	−8.66	−9.16
doxorubicin (positive control)	−7.27	−7.13	5.15
<i>N</i> -isopentyltridecanamide I–III	−6.20	−7.62	−8.68
eicosanamide	−6.98	−8.04	−6.88
methyl (2 <i>Z</i> ,6 <i>R</i> ,8 <i>S</i>)-4,6-diethyl-3,6-epoxy-8-methyldeca-2,4-dienoate I–II	−5.64	−7.72	−8.92
2,2'-bis(4-methyl-6- <i>tert</i> -butylphenol) methane I–II	−5.71	−7.22	−7.31
cis-11-eicosenamide I–III	−7.01	−7.92	−8.05
hydroxyleucine/hydroxyisoleucine	−4.51	−4.56	−5.35
<i>N</i> -methyl-D-glucosamine I–II	−4.99	−5.67	−6.10
hypotolide	−6.13	−7.68	−9.17
6-desmethyl-6-ethylspongisoritin A I–II	−5.75	−7.65	−8.36
8 α H,9 α H-11,12-diacetoxymirane	−5.40	−6.46	−7.26
bacillamadin G	−6.15	−7.37	−9.10
palmitamide I–II	−6.05	−7.41	−9.14

**Figure 12.** 2D interactions of (A) cocrystallized ligand (ABT-199), (B) doxorubicin (positive control), (C) *N*-isopentyltridecanamide I–III, (D) eicosanamide, (E) methyl (2*Z*,6*R*,8*S*)-4,6-diethyl-3,6-epoxy-8-methyldeca-2,4-dienoate I–II, (F) 2,2'-bis(4-methyl-6-*tert*-butylphenol)methane I–II, and (G) cis-11-eicosenamide I–III docked against BCL-2 PDB ID 4MAN.

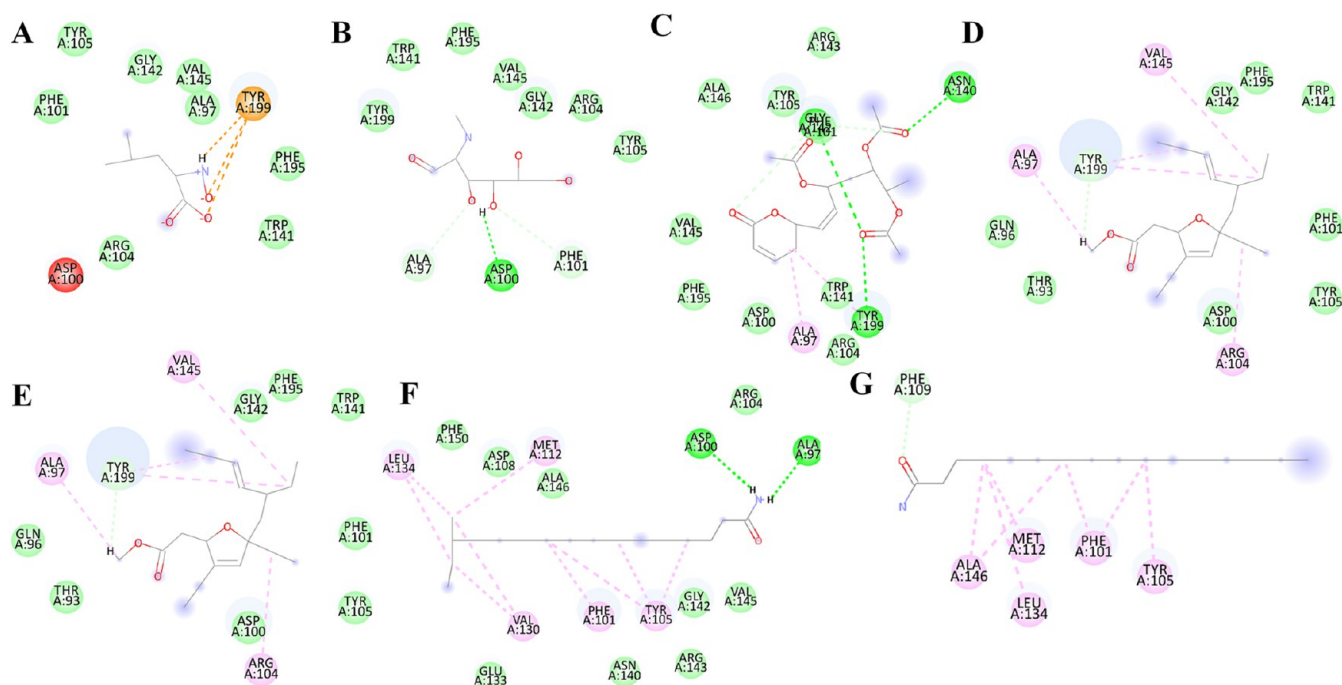


Figure 13. 2D interactions of (A) hydroxyleucine, (B) *N*-methyl-D-glucosamine I–II, (C) hyptolide, (D) 6-desmethyl-6-ethylspongisoritin A I–II, (E) 8aH,9aH-11,12-diacetoxymirane, (F) bacillamadin G, and (G) palmitamide I–II docked against BCL-2 PDB ID 4MAN.

lower than ABT-199, suggesting that additional interactions, such as ionic or hydrophobic interactions, are needed for stronger binding.

Bacillamadin G showed a moderate binding affinity (−6.15 kcal/mol), forming 2 H-bonds with Asp100 and Ala97 (Figure 13F). Although these H-bonds contribute to its binding affinity, the absence of additional interactions, such as ionic bonds or hydrophobic interactions, may have limited its binding potential. Palmitamide I–II displayed a binding affinity of −6.05 kcal/mol, relying solely on hydrophobic interactions similar to those of eicosanamide (Figure 13G). The lack of H-bonds or ionic interactions accounts for its lower binding affinity compared to other compounds that form more diverse interactions.

Overall, these results demonstrate that marine-derived compounds, particularly cis-11-eicosanamide and hyptolide, exhibit promising binding affinities to BCL-2, approaching those of the positive control, doxorubicin. The importance of H-bonding, particularly with key residues, such as Asp100 and Asp108, is highlighted as a critical factor in achieving strong binding to BCL-2. Additionally, hydrophobic interactions, while contributing to binding, appear to be less influential than H-bonds and ionic interactions in determining the binding strength.

The MCL-1-cocrystallized ligand, 2-indole-acylsulfonamide, exhibited a high binding affinity of −8.66 kcal/mol toward its receptor, with a low RMSD value of 1.62, validating the accuracy of the applied docking protocol (Table 2). The ligand formed two key hydrogen bonds (H-bonds) with the essential pocket residue Arg263 (Figure 14A). Doxorubicin, used as a positive control, also interacted with Arg263, forming one H-bond and two ionic interactions. Additionally, doxorubicin formed another H-bond with His224 and π - π stacking with Phe270, contributing to its binding affinity of −7.13 kcal/mol (Table 2 and Figure 14B).

Interestingly, nine components from the *E. asperum* and *C. siphonella* extracts demonstrated better binding affinities compared to doxorubicin. These compounds exhibited binding scores of −7.62, −8.04, −7.72, −7.22, −7.92, −7.68, −7.65, −7.37, and −7.41 kcal/mol for *N*-isopentyltridecanamide I–III, eicosanamide, methyl (2Z,6R,8S)-4,6-diethyl-3,6-epoxy-8-methyldeca-2,4-dienoate I–II, 2,2'-bis(4-methyl-6-*tert*-butylphenol), methane I–II, cis-11-eicosanamide I–III, hyptolide, 6-desmethyl-6-ethylspongisoritin A I–II, bacillamadin G, and palmitamide I–II, respectively (Table 2). Consistent with their behavior against BCL-2, both eicosanamide and cis-11-eicosanamide I–III showed the highest binding affinities against MCL-1. Eicosanamide predominantly relied on hydrophobic interactions within the MCL-1 binding pocket (Figure 14D), whereas cis-11-eicosanamide I–III formed an additional H-bond with Met250, enhancing its binding affinity (Figure 14G). *N*-Isopentyltridecanamide I–III and hyptolide also demonstrated strong interactions with MCL-1, forming H-bonds with the key residue Arg263, which plays a crucial role in stabilizing the complex (Figures 14C and 15C). In contrast, methyl (2Z,6R,8S)-4,6-diethyl-3,6-epoxy-8-methyldeca-2,4-dienoate I–II and 6-desmethyl-6-ethylspongisoritin A I–II, both furan derivatives, achieved high binding affinities through hydrophobic interactions within the MCL-1 pocket (Figures 14E and 15D). While bacillamadin G and palmitamide I–II also formed H-bonds within the MCL-1 binding pocket, their interactions were with His224 and Phe270 rather than with the key residue Arg263, which may explain their slightly lower binding affinities (Figure 15F,G). Nonetheless, the ability of these compounds to interact with MCL-1, particularly through H-bonds and hydrophobic interactions, highlights their potential as inhibitors of this antiapoptotic protein.

The cocrystallized ligand for estrogen receptor α (ER α), estradiol, demonstrated a strong binding affinity to its active site, with a binding energy of −9.16 kcal/mol and a very low RMSD of 0.14, confirming the reliability of the docking protocol (Table

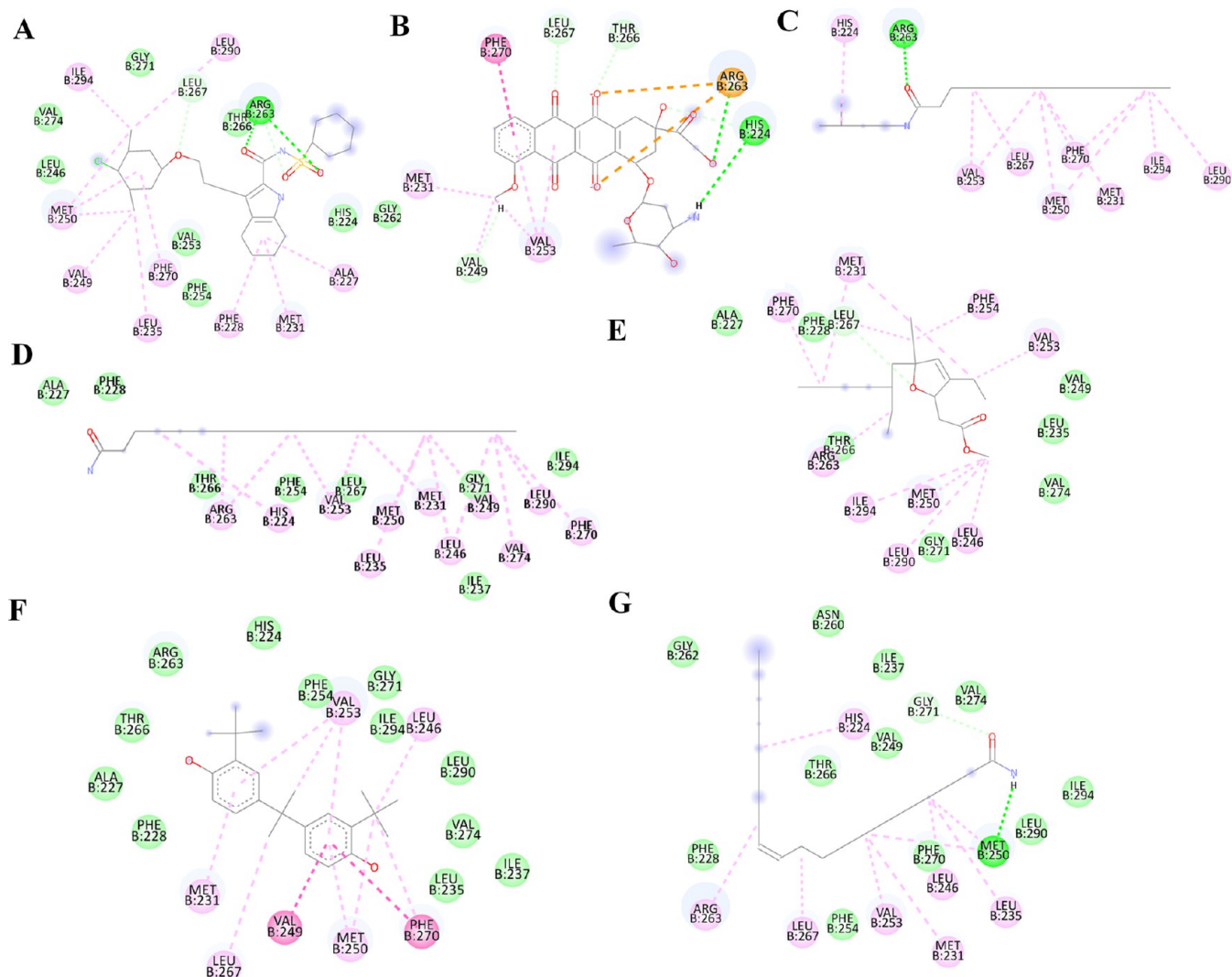


Figure 14. 2D interactions of (A) cocrystallized ligand (2-indole-acylsulfonamide), (B) doxorubicin (positive control), (C) *N*-isopentyltridecanamide I–III, (D) eicosanamide, (E) methyl (2Z,6R,8S)-4,6-diethyl-3,6-epoxy-8-methyldeca-2,4-dienoate I–II, (F) 2,2'-bis(4-methyl-6-*tert*-butylphenol)-methane I–II, and (G) *cis*-11-eicosanamide I–III docked against MCL-1 PDB ID 5FDO.

2). Estradiol formed two key hydrogen bonds (H-bonds) with His524 and Glu353, along with a pi–pi stacking interaction with Phe404, contributing to its stable binding (Figure 16A). However, doxorubicin could not bind effectively to the ER α receptor, exhibiting a highly positive binding energy due to unfavorable repulsions, particularly with Leu525 (Table 2 and Figure 16B). This suggests that doxorubicin is not a viable ligand for ER α .

Three major constituents of the extracts, hyptolide, bacillamidin G, and palmitamide, reported binding affinities comparable to that of the cocrystallized ligand. Hyptolide had the highest binding energy (-9.17 kcal/mol) and formed a H-bond with Leu525 (Figure 17C). Bacillamidin G displayed a binding energy of -9.10 kcal/mol with a H-bond formed between its amide group and Arg394 (Figure 17F). Palmitamide, which showed a binding affinity of -9.14 kcal/mol, relied entirely on hydrophobic interactions within the ER α binding pocket (Figure 17G). These interactions indicate that these components might effectively target ER α . Other constituents of the extracts, including *N*-isopentyltridecanamide I–III, methyl (2Z,6R,8S)-4,6-diethyl-3,6-epoxy-8-methyldeca-2,4-dienoate I–II, cis-11-eicosenamide I–III, and 6-desmethyl-

6-ethylspongosoritin A I–II, also exhibited significant binding affinities (greater than -8 kcal/mol) against ER α (Table 2). While *N*-isopentyltridecanamide I–III, cis-11-eicosenamide I–III, and 6-desmethyl-6-ethylspongosoritin relied solely on hydrophobic interactions (Figures 16C,G and 17D), methyl (2Z,6R,8S)-4,6-diethyl-3,6-epoxy-8-methyldeca-2,4-dienoate I–II formed an additional H-bond with Arg394, enhancing its binding stability (Figure 16E).

These findings highlight the potential of heptolide, bacillamidin G, and palmitamide as strong candidates for targeting ER α , given their ability to form critical interactions within the binding pocket akin to those of estradiol. Additionally, the hydrophobic interactions exhibited by other constituents, such as *N*-isopentyltridecanamide I–III and cis-11-eicosenamide I–III, further suggest that these extracts contain several bioactive compounds that may have therapeutic relevance in modulating ER α activity.

4. DISCUSSION

Breast cancer is one of the most prevalent cancers diagnosed in women worldwide, with incidence rates increasing in recent years. Although only a limited number of marine-derived drugs,

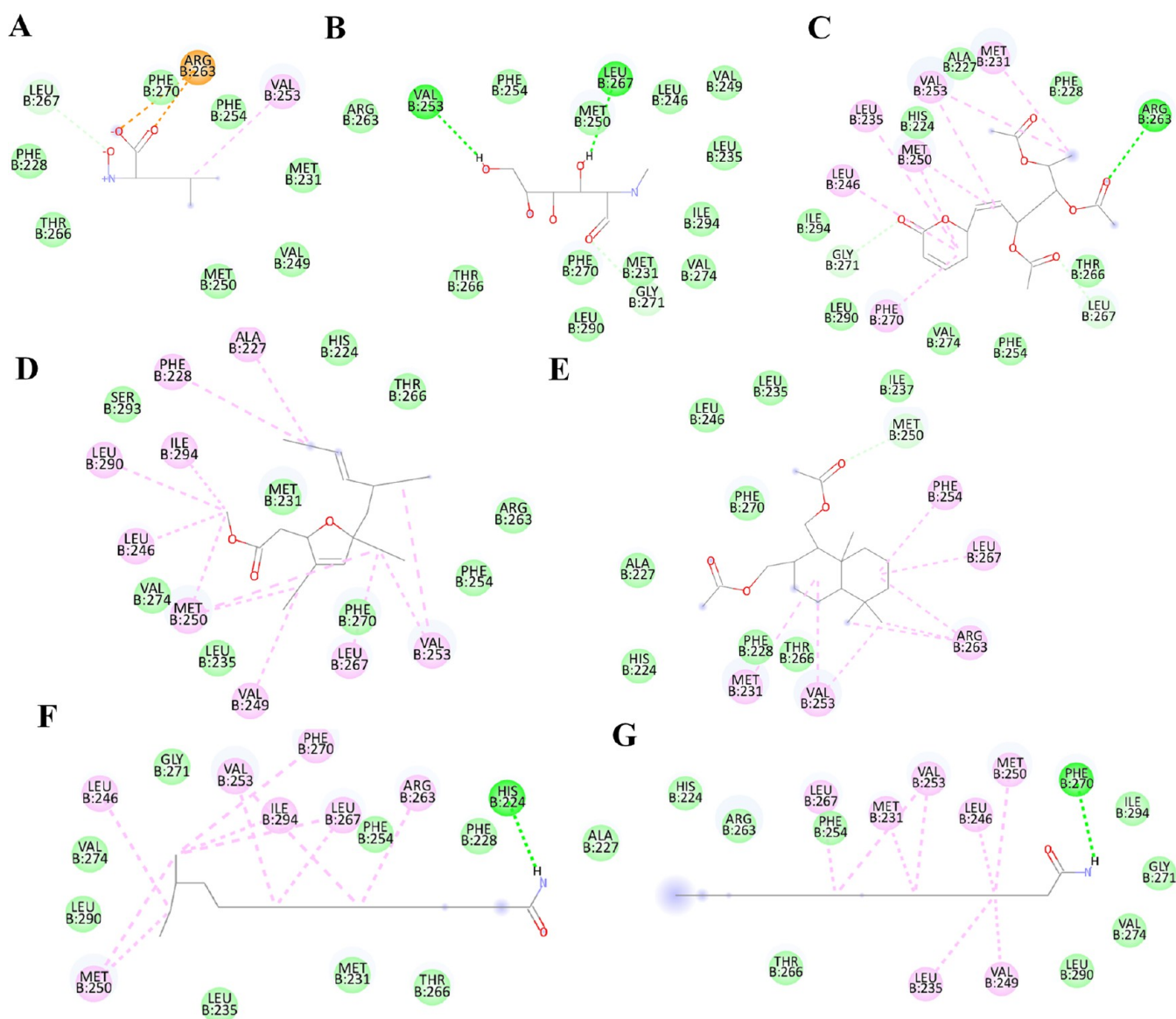


Figure 15. 2D interactions of (A) hydroxyleucine, (B) *N*-methyl-D-glucosamine I–II, (C) hyptolide, (D) 6-desmethyl-6-ethylspongisoritin A I–II, (E) 8 α H,9 α H-11,12-diacetoxydrimane, (F) bacillamidine G, and (G) palmitamide I–II docked against MCL-1 PDB ID 5FDO.

such as cytarabine (Cytosar-U) and trabectedin (Yondelis), are currently available for cancer treatment, over 20 additional marine compounds are undergoing phase II–III clinical trials (Figure 18).³⁵

Marine sponges (phylum Porifera) are ancient multicellular organisms that thrive in diverse aquatic environments. Their unique biology and symbiotic relationships with microorganisms enable them to produce a wide array of secondary metabolites including alkaloids, polyketides, terpenoids, peptides, and sterols. These metabolites exhibit various biological activities, particularly, anticancer properties. Several compounds isolated from marine sponges have been developed into FDA-approved drugs for cancer treatment, highlighting the significant therapeutic potential of marine biodiversity.³⁶ Cytarabine (Ara-C) is derived from the sponge *Cryptotethya crypta*. Cytarabine is crucial in treating certain leukemias, such as acute myeloid leukemia (AML) and non-Hodgkin's lymphoma, by acting as a nucleoside analog that inhibits DNA synthesis and induces cell death in rapidly dividing cells.³⁷

Another compound from *Cryptotethya crypta*, vidarabine (Ara-A), initially developed as an antiviral drug, has also shown significant antitumor activity through similar mechanisms (Figure 18).³⁸

Eribulin mesylate (Halaven), a synthetic derivative of halichondrin B from the sponge *Halichondria okadai*, exemplifies the unique mechanisms offered by marine-derived drugs. It inhibits microtubule dynamics during cell division, inducing apoptosis in cancer cells while sparing nondividing cells, thus reducing side effects compared to traditional chemotherapy (Figure 18).³⁹

Trabectedin (Yondelis), derived from the sea squirt *Ecteinascidia turbinata*, binds to DNA's minor groove and disrupts transcription processes vital for cancer cell survival. It has been approved for treating soft tissue sarcoma and relapsed ovarian cancer, demonstrating efficacy where conventional chemotherapy may fail.⁴⁰

Traditional chemotherapy has long been the mainstay of cancer treatment, but it often indiscriminately targets all rapidly dividing cells, leading to significant side effects due to toxicity to

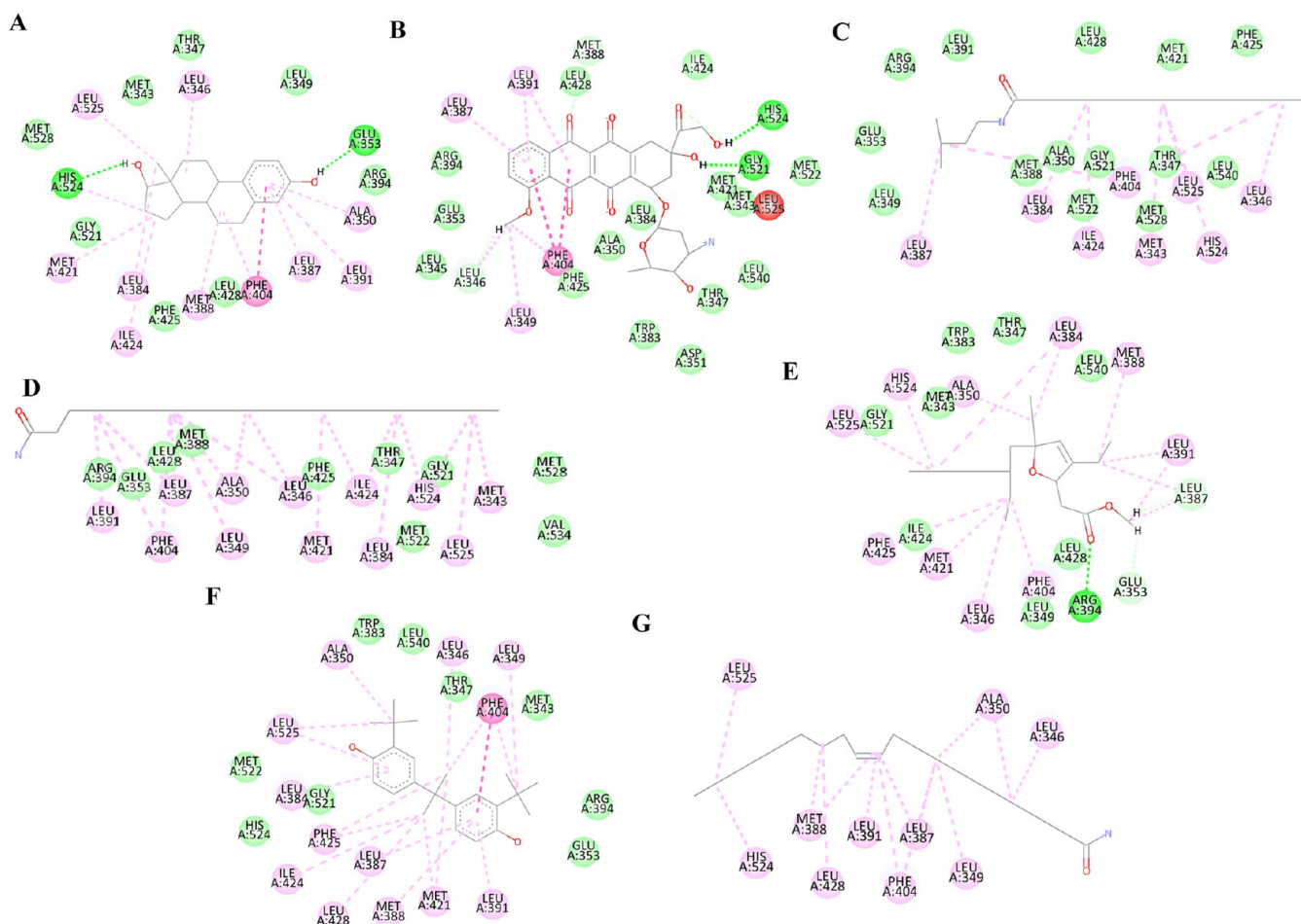


Figure 16. 2D interactions of (A) cocrystallized ligand (estradiol), (B) doxorubicin (positive control), (C) *N*-isopentyltridecanamide I–III, (D) eicosanamide, (E) methyl (2*Z*,6*R*,8*S*)-4,6-diethyl-3,6-epoxy-8-methyldeca-2,4-dienoate I–II, (F) 2,2'-bis(4-methyl-6-*tert*-butylphenol)methane I–II, and (G) *cis*-11-eicosenamide I–III docked against ER α PDB ID 1G50.

healthy tissues.⁴¹ In contrast, marine sponge-derived drugs present novel mechanisms that are more selective for cancer cells, potentially reducing collateral damage. For instance, cytarabine and vidarabine specifically inhibit DNA synthesis in rapidly dividing cells, making them particularly effective against hematological malignancies.^{37,38}

The key difference between traditional chemotherapy and marine sponge-derived drugs lies in their specificity and side effect profiles. Marine-derived drugs tend to target specific pathways or structures within cancer cells, minimizing harm to healthy cells and expanding treatment options for patients who do not respond to conventional therapies.⁴²

In this study, we evaluated the anticancer activity of methanolic extracts from *E. asperum* (EAE) and *C. siphonella* (CSE) on human breast cancer cell lines MCF-7 and MDA-MB-231. The IC₅₀ values indicated that EAE was more potent, with approximately 0.5 μ g/mL for MCF-7 cells and 8.7 μ g/mL for MDA-MB-231 cells, compared to CSE, which had IC₅₀ values of 2.7 and 45.3 μ g/mL, respectively. This demonstrates that EAE inhibits the growth of both breast cancer cell lines more effectively than CSE, requiring significantly lower concentrations for the same inhibitory effect, suggesting stronger cytotoxic properties for EAE.

Similarly, Ciftci et al.⁴³ reported that the ethanol extract of *Dysidea avara* shows IC₅₀ values of 11.51, 5.11, and 17.54 μ g/mL in the breast (MCF-7).

The results of the present investigation support these conclusions and highlight the cytotoxic effects of the CSE. The capacity of the CSE to activate autophagy in MDA-MB-231 cells is a noteworthy discovery that builds upon earlier research. The majority of research has been on cell cycle arrest and death; however, autophagy induction reveals the variety of ways that CSE metabolites prevent the development of cancer cells.¹⁸

The bioactivity of metabolites discovered in marine sponges, including fatty acids, terpenoids, alkaloids, long-chain amides, and sterols, significantly influences their therapeutic potential. Long-chain amides and lactones are particularly notable for their ability to disrupt cellular processes, leading to necrosis and apoptosis. These compounds can alter cell membrane composition and manipulate critical signaling pathways that are essential for cancer cell survival. Sterols enhance membrane fluidity and cellular signaling, demonstrating anticancer properties by inducing apoptosis and inhibiting cancer cell proliferation.^{19,44}

Fatty acids exhibit various biological actions, including anti-inflammatory and anticancer effects, by impacting cell signaling cascades and modifying cell membrane composition.⁴⁵ Terpenoids impede cancer cell growth and spread through their diverse biological activities, which encompass anti-inflammatory, anticancer, and antimicrobial effects.⁴⁶ Alkaloids are recognized for their strong biological effects, promoting apoptosis and inhibiting cell division in cancer cells.^{19,47}

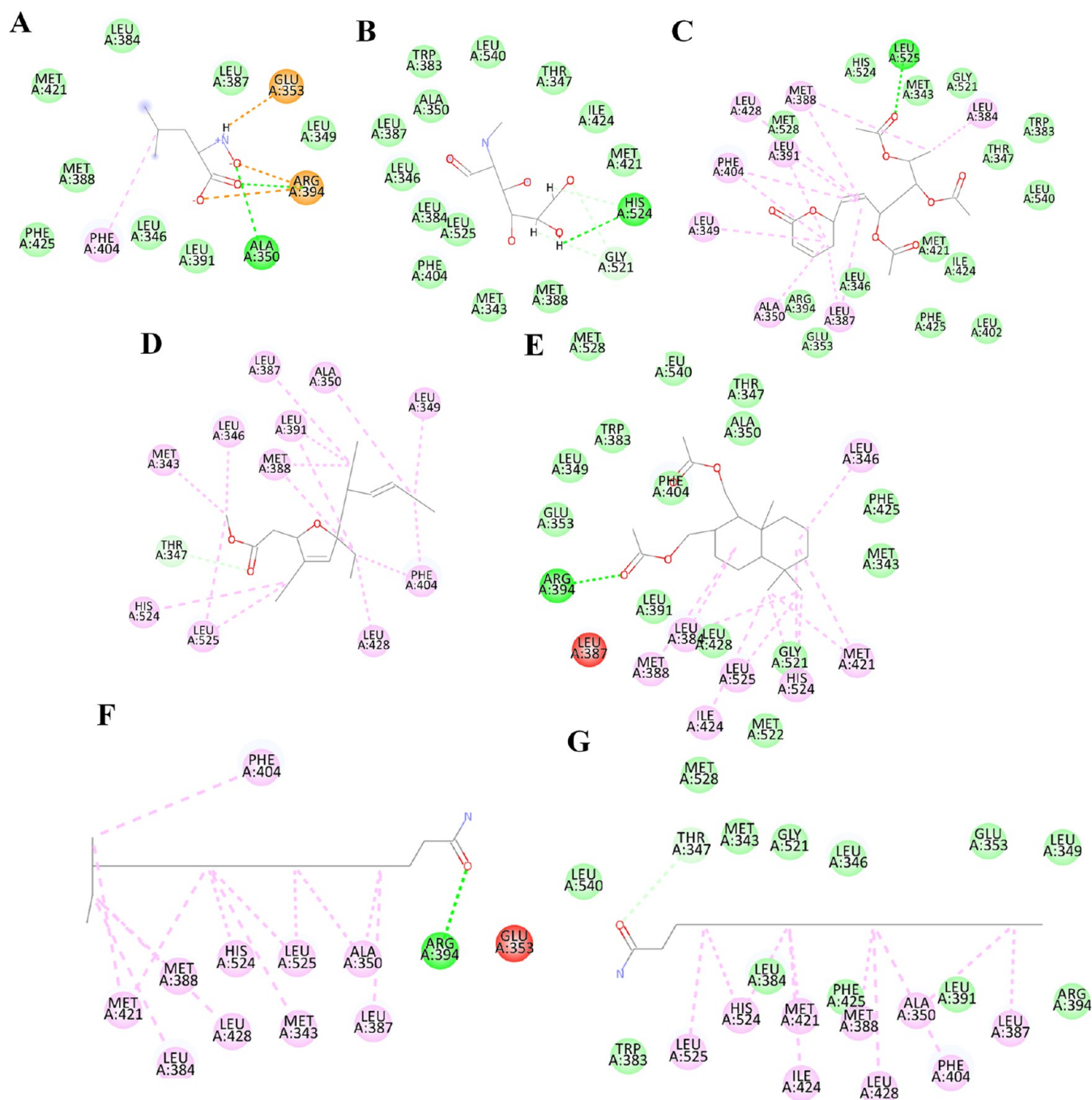


Figure 17. 2D interactions of (A) hydroxyleucine, (B) *N*-methyl-D-glucosamine I–II, (C) hyptolide, (D) 6-desmethyl-6-ethylspongosoritin A I–II, (E) 8α*H*,9α*H*-11,12-diacetoxymethane, (F) bacillamidine G, and (G) palmitamide I–II docked against ERα PDB ID 1G50.

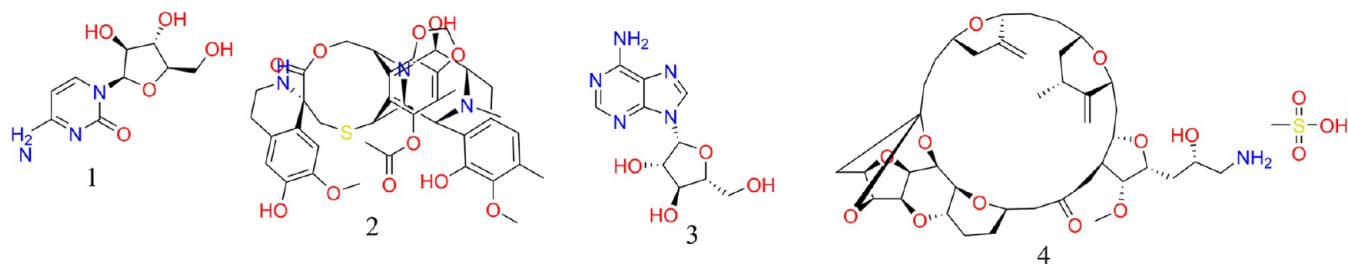


Figure 18. Chemical structures of anticancer marine-derived drugs (1) cytarabine, (2) trabectedin, (3) vidarabine, and (4) eribulin mesylate.

Comparative studies reveal interesting distinctions between the metabolites found in Red Sea sponges and those from other marine environments. For instance, the Mediterranean sponge *Aplysina aerophoba* has shown significant anticancer properties due to its unique secondary metabolites. These compounds share effective cytotoxic impacts with those identified in Red Sea sponges, disrupting various cellular processes in cancer cells.⁴⁸ Our findings align with previous research on marine sponge extracts. For example, researchers⁴⁹ reported that the ethyl acetate extract of *Spirastrella pachyspira* exhibited significant anticancer activity against the SKBR3 breast cancer cell line, with cell viability decreasing as the drug concentration increased. Similarly, studies by Malhão et al.⁵⁰ and Elissawy et al.⁵¹ have documented the cytotoxic effects of other marine sponges, reinforcing the potential of marine-derived compounds in cancer therapy.

Furthermore, EAE and CSE triggered apoptosis in human breast cancer cell lines at their respective IC₅₀ concentrations. Numerous studies have shown that anticancer drugs and chemopreventive agents often exert their effects by inducing apoptosis in various cancer cells. Additionally, the initiation of apoptosis is a common mechanism among many emerging anticancer agents.⁵²

As part of a preliminary investigation into the underlying mechanisms, the expression of several apoptosis-related genes was analyzed in MCF-7 and MDA-MB-231 cells treated with EAE and CSE at their IC₅₀ concentrations for 48 h. Activation of p53 in response to DNA damage resulted in cell cycle arrest and the inhibition of cell proliferation.⁵³ p53 functions as a sequence-specific binding protein and may be modulated by Bax, a member of the Bcl-2 family.^{54,55} The Bcl-2 family proteins are crucial regulators of apoptosis and include key antiapoptotic proteins, such as Bcl-xL and Bcl-2, as well as major proapoptotic proteins, like Bax and Bak.⁵⁶ Studies have shown that increased Bax expression due to p53 overexpression is associated with the induction of apoptosis in various cell types.^{54,57}

Cell cycle arrest is one of the mechanisms that is looked at during the development of an anticancer drug. Several reports have shown the potential anticancer effect of sponge-based derivatives on the cell cycle.^{19,58}

Given that EAE and CSE were effective in inhibiting cell viability, we examined their effect on cell cycle arrest. The results showed that at concentrations of 0.5 μ g/mL EAE and 2.7 μ g/mL CSE, there is interference with cell cycle distribution in a dose-dependent manner. Compared to the untreated control, EAE exhibited an antiproliferative effect by arresting the cell cycle of MCF-7 cell lines in the G2 phase, while CSE significantly increased the cell population in the S phase. In MDA-MB-231 cell lines, treatment with both EAE and CSE resulted in a significant increase in the cell population in the S phase, demonstrating a strong antiproliferative effect compared to untreated cells.

Similarly, Lin et al.⁵⁹ demonstrated that API induced cell cycle arrest at the G2/M phase in MDA-MB-231 cells and at the G0/G1 phase in MCF-7 cells. Additionally, Tsuboy et al.⁶⁰ reported that GEN, at concentrations of 10 and 25 μ M, arrested MCF-7 cells in the G0/G1 phase. These findings contrast with our observations despite the higher concentrations used in their study.

Our study demonstrates that treatment with sponge extracts EAE and CSE induces autophagy in MDA-MB-231 breast cancer cells but not in MCF-7 cells. This cell-line-specific response highlights the nuanced effects of these extracts on

different cancer cell types. The study investigates the induction of autophagy by sponge extracts EAE and CSE in breast cancer cell lines MCF-7 and MDA-MB-231. Autophagy, a cellular degradation process, is crucial for maintaining cellular homeostasis, especially under stress conditions. To assess autophagy induction, the presence of acidic vesicular organelles (AVOs) was detected using acridine orange staining, which specifically stains acidic compartments, such as autophagic vacuoles. The stained cells were then analyzed via flow cytometry.

In MCF-7 cells, treatment with EAE (0.5 μ g/mL) and CSE (2.7 μ g/mL) did not significantly alter the percentage of autophagic cells. This lack of response indicates that these sponge extracts do not induce autophagy in MCF-7 cells under the tested conditions. The absence of a significant increase in the level of AVOs suggests that the extracts might not be effective in triggering the autophagic pathway in this particular cell line. In contrast, MDA-MB-231 cells exhibited a notable increase in autophagic cell formation upon treatment with the same concentrations of EAE and CSE. This observation implies a cell-line-specific response where MDA-MB-231 cells are more susceptible to autophagy induction by the sponge extracts. The significant increase in the number of AVOs indicates that these cells respond to the extracts by enhancing the autophagic process.

The results highlight a differential response to sponge extracts among the two breast cancer cell lines. MDA-MB-231 cells, which are known to be more aggressive and invasive compared to MCF-7 cells, showed a pronounced autophagic response. This suggests that the cellular context, including genetic and molecular differences between the cell lines, plays a crucial role in determining the efficacy of autophagy induction by the sponge extracts.

The heightened autophagic response in MDA-MB-231 cells could be associated with the extracts' potential therapeutic effects. Autophagy can have dual roles in cancer; it can promote cell survival under stress or lead to autophagic cell death. Understanding the exact mechanism and outcome of autophagy induction in MDA-MB-231 cells requires further investigation.

Similar findings have been reported in recent studies investigating the effects of natural compounds on autophagy. For instance, ref 61 showed that a marine sponge-derived compound induced autophagy in various cancer cell lines, with a pronounced effect in triple-negative breast cancer cells (MDA-MB-231), but not in hormone receptor-positive cells like MCF-7. This suggests that the cellular context, including genetic and molecular characteristics, significantly influences the autophagic response to treatment.

The increased autophagic response observed in MDA-MB-231 cells in our study is also consistent with the findings of ref 62, who reported that stress conditions, such as treatment with cytotoxic agents, often result in enhanced autophagy in more aggressive and less differentiated cancer cell lines. This may suggest a survival mechanism that can be therapeutically targeted.

We now have evidence that marine sponge-derived chemicals can alter autophagic pathways, suggesting a possible cancer subtype treatment. We show that these chemicals can induce autophagy and reduce cancer cell proliferation, bypassing cancer therapy resistance pathways. This research emphasizes marine biodiversity as a source of novel bioactive chemicals and the therapeutic potential of natural products in the development of more effective and tailored cancer treatments. Thus, more research into these chemicals' molecular processes and clinical

uses is needed to develop effective treatments for hard-to-treat tumors.

5. CONCLUSIONS

Our findings underscore the potential of marine sponges as a valuable source of potent anticancer agents. The extracts from CSE and EAE demonstrated significant inhibition of cellular proliferation, exhibited strong cytotoxic effects, and effectively induced apoptosis in human breast cancer cell lines. We propose that the mechanism underlying apoptosis induction by CSE and EAE likely involves a p53-dependent pathway, which is critical for regulating the cell cycle and promoting programmed cell death in response to cellular stress.

The ability of these extracts to induce apoptosis suggests that they may offer a novel strategy for cancer chemotherapy, potentially providing new avenues for treatment in breast cancer patients, especially those with p53 mutations or dysfunctions. Furthermore, the phytochemical analysis of both EAE and CSE revealed a diverse array of bioactive metabolites mostly described for the first time in EAE and CSE, indicating rich potential for therapeutic development.

To complement our findings, molecular docking studies were conducted to assess the binding affinity of the identified bioactive metabolites for key targets involved in cancer progression and survival, specifically BCL-2, MCL-1, and ER α . Preliminary results suggest that several compounds within the extracts exhibit strong binding affinities for these targets. However, further research is necessary to establish a standardized method for extracting and characterizing these metabolites. By elucidating the mechanisms of action and optimizing delivery methods, we aim to pave the way for the development of innovative anticancer therapies derived from marine sponge sources.

■ ASSOCIATED CONTENT

Data Availability Statement

All data are available within the manuscript.

SI Supporting Information

The Supporting Information is available free of charge at <https://pubs.acs.org/doi/10.1021/acsomega.4c10202>.

2D chemical structure of *Echinodictyum asperum* and *Callyspongia siphonella* major extracts' constituents (Table S1) (PDF)

■ AUTHOR INFORMATION

Corresponding Author

Reham Hassan Mekky – Department of Pharmacognosy, Faculty of Pharmacy, Egyptian Russian University, Cairo 11829, Egypt; orcid.org/0000-0001-5613-5666; Email: reham-mekky@eru.edu.eg

Authors

Samah S. Abuzahrah – Department of Biological Sciences, College of Science, University of Jeddah, Jeddah 21959, Saudi Arabia

Tahani Bakhsh – Department of Biological Sciences, College of Science, University of Jeddah, Jeddah 21959, Saudi Arabia

Serag Eldin I. Elbehairi – Faculty of Science, Biology Department, King Khalid University, Abha 9004, Saudi Arabia; Tissue Culture and Cancer Biology Research Laboratory, King Khalid University, Abha 9004, Saudi Arabia

Nouf Juaid – Basic Medical Science Department, Inaya Medical College, Riyadh 12211, Saudi Arabia

Complete contact information is available at:

<https://pubs.acs.org/doi/10.1021/acsomega.4c10202>

Author Contributions

#S.S.A. and N.J. contributed equally to this work. Study design was done by S.S.A., T.B., R.H.M., S.I.E., and N.J. The experiments and statistical analysis were carried out by S.S.A., T.B., R.H.M., S.I.E., and N.J. Resources and methodological assistance were provided by S.S.A., T.B., R.H.M., S.I.E., and N.J. The original draft of the manuscript was written by S.S.A., T.B., R.H.M., S.I.E., and N.J. All authors then edited and accepted the updated version of the article. Each author has reviewed the published version of the manuscript and given their approval.

Funding

This work was funded by the University of Jeddah, Jeddah, Saudi Arabia, under grant No. (UJ-23-SRP-5). The authors, therefore, thank the University of Jeddah for its technical and financial support.

Notes

The authors declare no competing financial interest.

■ ACKNOWLEDGMENTS

The authors acknowledge the efforts of Kamal Al-Dahood.

■ REFERENCES

- (1) Nolan, E.; Lindeman, G. J.; Visvader, J. E. Deciphering breast cancer: from biology to the clinic. *Cell* **2023**, 186 (8), 1708–1728.
- (2) Yang, G.-J.; Song, Y.-Q.; Wang, W.; Han, Q.-B.; Ma, D.-L.; Leung, C.-H. An optimized BRD4 inhibitor effectively eliminates NF- κ B-driven triple-negative breast cancer cells. *Bioorg. Chem.* **2021**, 114, No. 105158.
- (3) Cheng, S.; Yang, G.-J.; Wang, W.; Ma, D.-L.; Leung, C.-H. Discovery of a tetrahydroisoquinoline-based CDK9-cyclin T1 protein–protein interaction inhibitor as an anti-proliferative and anti-migration agent against triple-negative breast cancer cells. *Genes Dis.* **2022**, 9 (6), 1674–1688.
- (4) Cheng, S.-S.; Qu, Y.-Q.; Wu, J.; Yang, G.-J.; Liu, H.; Wang, W.; Huang, Q.; Chen, F.; Li, G.; Wong, C.-Y.; et al. Inhibition of the CDK9–cyclin T1 protein–protein interaction as a new approach against triple-negative breast cancer. *Acta Pharm. Sin. B* **2022**, 12 (3), 1390–1405.
- (5) Min, J.; Nwachukwu, J. C.; Min, C. K.; Njeri, J. W.; Srinivasan, S.; Rangarajan, E. S.; Nettles, C. C.; Sanabria Guillen, V.; Ziegler, Y.; Yan, S.; et al. Dual-mechanism estrogen receptor inhibitors. *Proc. Natl. Acad. Sci. U.S.A.* **2021**, 118 (35), No. e2101657118.
- (6) Hassanin, S. O.; Hegab, A. M. M.; Mekky, R. H.; Said, M. A.; Khalil, M. G.; Hamza, A. A.; Amin, A. Combining In Vitro, In Vivo, and Network Pharmacology Assays to Identify Targets and Molecular Mechanisms of Spirulina-Derived Biomolecules against Breast Cancer. *Mar. Drugs* **2024**, 22 (7), 328.
- (7) Mohammed, R.; Seliem, M. A. E.; Mohammed, T.; Abed-El Fatah, A.; Abo-Youssef, A.; Thabet, M. Bioactive secondary metabolites from the Red Sea soft coral *Heteroxenia fuscens*. *Int. J. Appl. Res. Nat. Prod* **2012**, 4 (4), 15–27.
- (8) Nandi, S.; Khatua, S.; Nag, A.; Sen, S.; Chakraborty, N.; Naskar, A.; Acharya, K.; Mekky, R. H.; Contreras, M. d. M.; Calina, D.; et al. Dolastatins and their analogues present a compelling landscape of potential natural and synthetic anticancer drug candidates. *Curr. Res. Biotechnol.* **2024**, 7, No. 100167.
- (9) Calabrin, C.; Catanzaro, E.; Bishayee, A.; Turrini, E.; Fimognari, C. Marine sponge natural products with anticancer potential: An updated review. *Mar. Drugs* **2017**, 15 (10), 310.
- (10) Van Soest, R. W. M.; Boury-Esnault, N.; Vacelet, J.; Dohrmann, M.; Erpenbeck, D.; De Voogd, N. J.; Santodomingo, N.; Vanhoorne, B.; Kelly, M.; Hooper, J. N. A. Global Diversity of Sponges (Porifera). *PLoS One* **2012**, 7 (4), No. e35105.

- (7) Kumar, M. S.; Adki, K. M. Marine natural products for multi-targeted cancer treatment: A future insight. *Biomed. Pharmacother.* **2018**, *105*, 233–245.
- (8) Ruiz-Torres, V.; Encinar, J. A.; Herranz-Lopez, M.; Perez-Sanchez, A.; Galiano, V.; Barrajon-Catalan, E.; Micol, V. An updated review on marine anticancer compounds: The use of virtual screening for the discovery of small-molecule cancer drugs. *Molecules* **2017**, *22* (7), 1037.
- (9) World Porifera Database. *Echinodictyum asperum* Ridley & Dendy, 1886. <https://www.marinespecies.org/aphia.php?p=taxdetails&id=167963>.
- (10) Ridley, S. O.; Dendy, A. Preliminary report on the Monaxonida collected by H.M.S. Challenger. Part I. *Ann. Mag. Nat. Hist.* **1886**, *18*, 470–493.
- (11) Ovenden, S. P. B.; Capon, R. J. Echinodictyum A–C and Echinodictyum A: Novel Bromoindole Sulfonic Acids and a Sulfone from a Southern Australian Marine Sponge, *Echinodictyum*. *J. Nat. Prod.* **1999**, *62* (9), 1246–1249.
- (12) Capon, R. J.; Vuong, D.; Lacey, E.; Gill, J. H. (–)-Echinobetaine A: Isolation, Structure Elucidation, Synthesis, and SAR Studies on a New Nematocide from a Southern Australian Marine Sponge, *Echinodictyum* sp. *J. Nat. Prod.* **2005**, *68* (2), 179–182. Capon, R. J.; Vuong, D.; McNally, M.; Peterle, T.; Trotter, N.; Lacey, E.; Gill, J. H. (+)-Echinobetaine B: isolation, structure elucidation, synthesis and preliminary SAR studies on a new nematocidal betaine from a southern Australian marine sponge, *Echinodictyum* sp. *Org. Biomol. Chem.* **2005**, *3* (1), 118–122.
- (13) MarinLit, 2024. <https://marinlit.rsc.org>.
- (14) de Sousa, L. H. N.; de Araújo, R. D.; Sousa-Fontoura, D.; Menezes, F. G.; Araújo, R. M. Metabolites from Marine Sponges of the Genus *Callyspongia*: Occurrence, Biological Activity, and NMR Data. *Mar. Drugs* **2021**, *19* (12), 663.
- (15) Hadisaputri, Y. E.; Nurhaniefah, A. A.; Sukmara, S.; Zuhrotun, A.; Hendriani, R.; Sopyan, I. *Callyspongia* spp.: Secondary Metabolites, Pharmacological Activities, and Mechanisms. *Metabolites* **2023**, *13* (2), 217.
- (16) Jain, S.; Shirode, A.; Yacoub, S.; Barbo, A.; Sylvester, P. W.; Huntimer, E.; Halaweish, F.; El Sayed, K. A. Biocatalysis of the anticancer siphonane triterpenoids. *Planta Med.* **2007**, *73* (06), 591–596.
- (17) Jain, S.; Laphookhieo, S.; Shi, Z.; Fu, L.-w.; Akiyama, S.-i.; Chen, Z.-S.; Youssef, D. T. A.; van Soest, R. W. M.; El Sayed, K. A. Reversal of P-Glycoprotein-Mediated Multidrug Resistance by Siphonane Triterpenoids. *J. Nat. Prod.* **2007**, *70* (6), 928–931.
- (18) El-Naggar, H. A.; Bashar, M. A.; Rady, I.; El-Wetidy, M. S.; Suleiman, W. B.; Al-Otibi, F. O.; Al-Rashed, S. A.; Abd El-Maoula, L. M.; Salem, E.-S. S.; Attia, E. M.; Bakry, S. Two red sea sponge extracts (*Negombata magnifica* and *Callyspongia siphonella*) induced anticancer and antimicrobial activity. *Appl. Sci.* **2022**, *12* (3), 1400. El-Hawary, S. S.; Sayed, A. M.; Mohammed, R.; Hassan, H. M.; Rateb, M. E.; Amin, E.; Mohammed, T. A.; El-Mesury, M.; Bin Muhsinah, A.; Alsayari, A.; et al. Bioactive brominated oxindole alkaloids from the Red Sea sponge *Callyspongia siphonella*. *Mar. Drugs* **2019**, *17* (8), 465.
- (19) El-Demerdash, A.; Tammam, M. A.; Atanasov, A. G.; Hooper, J. N.; Al-Mourabit, A.; Kijjoa, A. Chemistry and biological activities of the marine sponges of the genera *Mycale* (Arenochalina), *Biemna* and *Clathria*. *Mar. Drugs* **2018**, *16* (6), 214.
- (20) Frstiohad, A.; Sadarun, B.; Bafadal, M.; Andriani, R.; Purnama, L.; Malik, F.; Ilyas, M.; Malaka, M.; Sahidin, I. Pharmacological Activity of Compounds Isolated from Methanolic Extract Marine Sponge *Xestospongia* sp. Against *Escherichia coli* and *Staphylococcus aureus*. In *Journal of Physics: Conference Series*; IOP Publishing, 2021; Vol. 1899, p 012048.
- (21) Sweilam, S. H.; Abd El Hafeez, M. S.; Mansour, M. A.; Mekky, R. H. Unravelling the Phytochemical Composition and Antioxidant Potential of Different Parts of *Rumex vesicarius* L.: A RP-HPLC-MS-MS/MS, Chemometrics, and Molecular Docking-Based Comparative Study. *Plants* **2024**, *13* (13), 1815.
- (22) Saeed, N. M.; Ramadan, L. A.; El-Sabbagh, W. A.; Said, M. A.; Abdel-Rahman, H. M.; Mekky, R. H. Exploring the anti-osteoporosis potential of *Petroselinum crispum* (Mill.) Fuss extract employing experimentally ovariectomized rat model and network pharmacology approach. *Fitoterapia* **2024**, *175*, No. 105971.
- (23) Reaxys, 2024. <http://www.reaxys.com>.
- (24) Tej, A.; Mekky, R. H.; Contreras, M. d. M.; Feriani, A.; Tir, M.; L'Taief, B.; Alshaharni, M. O.; Faidi, B.; Mnafigui, K.; Abbes, Z.; et al. *Eucalyptus torquata* seeds: Investigation of phytochemicals profile via LC-MS and its potential cardiopreventive capacity in rats. *Food Biosci.* **2024**, *59*, No. 103666.
- (25) Mekky, R. H.; Abdel-Sattar, E.; Abdulla, M.-H.; Segura-Carretero, A.; Al-Khayal, K.; Eldehna, W. M.; del Mar Contreras, M. Metabolic profiling and antioxidant activity of fenugreek seeds cultivars 'Giza 2' and 'Giza 30' compared to other geographically-related seeds. *Food Chem.: X* **2024**, *24*, No. 101819.
- (26) Thomas, L. W.; Lam, C.; Edwards, S. W. Mcl-1; the molecular regulation of protein function. *FEBS Lett.* **2010**, *584* (14), 2981–2989.
- (27) Ali, S.; Coombes, R. C. Endocrine-responsive breast cancer and strategies for combating resistance. *Nat. Rev. Cancer.* **2002**, *2* (2), 101–112.
- (28) Berman, H. M.; Westbrook, J.; Feng, Z.; Gilliland, G.; Bhat, T. N.; Weissig, H.; Shindyalov, I. N.; Bourne, P. E. The protein data bank. *Nucleic Acids Res.* **2000**, *28* (1), 235–242.
- (29) Morris, G.; Huey, R.; Lindstrom, W.; Sanner, M.; Belew, R.; Goodsell, D. AutoDockTools4: Automated docking with selective receptor flexibility. *J. Comput. Chem.* **2009**, *30*, 2785–2791.
- (30) Gasteiger, J.; Marsili, M. Iterative partial equalization of orbital electronegativity—a rapid access to atomic charges. *Tetrahedron* **1980**, *36* (22), 3219–3228.
- (31) Bitencourt-Ferreira, G.; Pintro, V. O.; de Azevedo, W. F. Docking with autodock4. In *Docking Screens for Drug Discovery*; Springer, 2019; Vol. 2053, pp 125–148.
- (32) Kontoyianni, M. Docking and Virtual Screening in Drug Discovery. In *Proteomics for Drug Discovery: Methods and Protocols*; Springer, 2017; Vol. 1647, pp 255–266.
- (33) Mekky, R. H.; Abdel-Sattar, E.; Segura-Carretero, A.; Contreras, M. d. M. A comparative study on the metabolites profiling of linseed cakes from Egyptian cultivars and antioxidant activity applying mass spectrometry-based analysis and chemometrics. *Food Chem.* **2022**, *395*, No. 133524.
- (34) Aly, O.; Mekky, R. H.; Pereira, F.; Diab, Y. M.; Tammam, M. A.; El-Demerdash, A. Deciphering the potential of *Cymbopogon citratus* (DC.) Stapf as an anti-obesity agent: phytochemical profiling, in vivo evaluations and molecular docking studies. *Food Funct.* **2024**, *15* (24), 12146–12168.
- (35) Jimenez, P. C.; Wilke, D. V.; Costa-Lotufo, L. V. Marine drugs for cancer: Surfacing biotechnological innovations from the oceans. *Clinics* **2018**, *73* (1), No. e482s.
- (36) Hooper, J.; Capon, R.; Keenan, C.; Parry, D.; Smit, N. Chemotaxonomy of marine sponges: Families Microcionidae, Raspailiidae and Axinellidae, and their relationships with other families in the orders Poecilosclerida and Axinellida (Porifera: Demospongiae). *Invertebr. Syst.* **1992**, *6* (2), 261–301.
- (37) El-Subbagh, H. I.; Al-Badr, A. A. Cytarabine. In *Profiles of Drug Substances, Excipients and Related Methodology*; Elsevier, 2009; Vol. 34, pp 37–113.
- (38) Whitley, R.; Alford, C.; Hess, F.; Buchanan, R. Vidarabine: a preliminary review of its pharmacological properties and therapeutic use. *Drugs* **1980**, *20*, 267–282.
- (39) Menis, J.; Twelves, C. Eribulin (Halaven): a new, effective treatment for women with heavily pretreated metastatic breast cancer. *Breast Cancer: Targets Ther.* **2011**, 101–111.
- (40) Larsen, A. K.; Galmarini, C. M.; D'Incalci, M. Unique features of trabectedin mechanism of action. *Cancer Chemother. Pharmacol.* **2016**, *77*, 663–671.
- (41) Chabner, B. A.; Roberts, T. G., Jr Chemotherapy and the war on cancer. *Nat. Rev. Cancer* **2005**, *5* (1), 65–72.
- (42) Ratan, R.; Patel, S. R. Trabectedin and eribulin: where do they fit in the management of soft tissue sarcoma? *Curr. Treat. Options Oncol.* **2017**, *18*, 1–9.

- (43) Ciftci, H. I.; Can, M.; Ellakwa, D. E.; Suner, S. C.; Ibrahim, M. A.; Oral, A.; Sekeroglu, N.; Özalp, B.; Otsuka, M.; Fujita, M.; et al. Anticancer activity of Turkish marine extracts: A purple sponge extract induces apoptosis with multitarget kinase inhibition activity. *Invest. New Drugs* **2020**, *38*, 1326–1333.
- (44) Heidary Jamebozorgi, F.; Yousefzadi, M.; Firuzi, O.; Nazemi, M.; Jassbi, A. R. In vitro anti-proliferative activities of the sterols and fatty acids isolated from the Persian Gulf sponge; *Axinella sinoxea*. *DARU J. Pharm. Sci.* **2019**, *27* (1), 121–135. Zhang, C.; Yu, H.; Shen, Y.; Ni, X.; Shen, S.; Das, U. N. Polyunsaturated fatty acids trigger apoptosis of colon cancer cells through a mitochondrial pathway. *Arch. Med. Sci.* **2015**, *11* (5), 1081–1094. From NLM
- (45) Hagve, T.-A. Effects of unsaturated fatty acids on cell membrane functions. *Scand. J. Clin. Lab. Invest.* **1988**, *48* (5), 381–388.
- (46) Kuttan, G.; Pratheeshkumar, P.; Manu, K. A.; Kuttan, R. Inhibition of tumor progression by naturally occurring terpenoids. *Pharm. Biol.* **2011**, *49* (10), 995–1007.
- (47) Mondal, A.; Gandhi, A.; Fimognari, C.; Atanasov, A. G.; Bishayee, A. Alkaloids for cancer prevention and therapy: Current progress and future perspectives. *Eur. J. Pharmacol.* **2019**, *858*, No. 172472.
- (48) Martínez-Poveda, B.; Medina, M. Á.; Quesada, A. R. Aerolysin-1, A Sponge-Derived Compound with Multi-Target Biological Activity. *Encyclopedia Mar. Biotechnol.* **2020**, *3*, 1351–1368.
- (49) Morais, S. R.; K, C.; Jeyabalan, S.; Wong, L. S.; Sekar, M.; Chidambaram, K.; Gan, S. H.; Begum, M. Y.; Izzati Mat Rani, N. N.; Subramaniyan, V.; et al. Anticancer potential of *Spirastrella pachyspira* (marine sponge) against SK-BR-3 human breast cancer cell line and in silico analysis of its bioactive molecule sphingosine. *Front. Mar. Sci.* **2022**, *9*, No. 950880, DOI: 10.3389/fmars.2022.950880.
- (50) Malhão, F.; Ramos, A. A.; Buttachon, S.; Dethoup, T.; Kijjoa, A.; Rocha, E. Cytotoxic and antiproliferative effects of preussin, a hydroxypyrrrolidine derivative from the marine sponge-associated fungus *Aspergillus candidus* KUFA 0062, in a panel of breast cancer cell lines and using 2D and 3D cultures. *Mar. Drugs* **2019**, *17* (8), 448.
- (51) Elissawy, A. M.; Soleiman Dehkordi, E.; Mehdinezhad, N.; Ashour, M. L.; Mohammadi Pour, P. Cytotoxic alkaloids derived from marine sponges: A comprehensive review. *Biomolecules* **2021**, *11* (2), 258.
- (52) Hersey, P.; Zhang, X. D. Overcoming resistance of cancer cells to apoptosis. *J. Cell. Physiol.* **2003**, *196* (1), 9–18. Tsuruo, T.; Naito, M.; Tomida, A.; Fujita, N.; Mashima, T.; Sakamoto, H.; Haga, N. Molecular targeting therapy of cancer: drug resistance, apoptosis and survival signal. *Cancer Sci.* **2003**, *94* (1), 15–21.
- (53) Lepik, D.; Jaks, V.; Kadaja, L.; Värvi, S.; Maimets, T. Electroporation and carrier DNA cause p53 activation, cell cycle arrest, and apoptosis. *Anal. Biochem.* **2003**, *318* (1), 52–59. Liebermann, D. A.; Hoffman, B.; Steinman, R. A. Molecular controls of growth arrest and apoptosis: p53-dependent and independent pathways. *Oncogene* **1995**, *11* (1), 199–210.
- (54) McCurrach, M. E.; Connor, T. M.; Knudson, C. M.; Korsmeyer, S. J.; Lowe, S. W. bax-deficiency promotes drug resistance and oncogenic transformation by attenuating p53-dependent apoptosis. *Proc. Natl. Acad. Sci. U.S.A.* **1997**, *94* (6), 2345–2349.
- (55) Selvakumaran, M.; Lin, H.-K.; Miyashita, T.; Wang, H. G.; Krajewski, S.; Reed, J. C.; Hoffman, B.; Liebermann, D. Immediate early up-regulation of bax expression by p53 but not TGF beta 1: a paradigm for distinct apoptotic pathways. *Oncogene* **1994**, *9* (6), 1791–1798.
- (56) Llambi, F.; Green, D. R. Apoptosis and oncogenesis: give and take in the BCL-2 family. *Curr. Opin. Genet. Dev.* **2011**, *21* (1), 12–20.
- (57) Miyashita, T.; Krajewski, S.; Krajewska, M.; Wang, H. G.; Lin, H.; Liebermann, D. A.; Hoffman, B.; Reed, J. C. Tumor suppressor p53 is a regulator of bcl-2 and bax gene expression in vitro and in vivo. *Oncogene* **1994**, *9* (6), 1799–1805.
- (58) Ebada, S. S.; Lin, W.; Proksch, P. Bioactive sesterterpenes and triterpenes from marine sponges: Occurrence and pharmacological significance. *Mar. Drugs* **2010**, *8* (2), 313–346. Varijakzhan, D.; Loh, J.-Y.; Yap, W.-S.; Yusoff, K.; Seboussi, R.; Lim, S.-H. E.; Lai, K.-S.; Chong, C.-M. Bioactive compounds from marine sponges: Fundamentals and applications. *Mar. Drugs* **2021**, *19* (5), 246.
- (59) Lin, N. U.; Vanderplas, A.; Hughes, M. E.; Theriault, R. L.; Edge, S. B.; Wong, Y. N.; Blayney, D. W.; Niland, J. C.; Winer, E. P.; Weeks, J. C. Clinicopathologic features, patterns of recurrence, and survival among women with triple-negative breast cancer in the National Comprehensive Cancer Network. *Cancer* **2012**, *118* (22), 5463–5472.
- (60) Tsuboy, M. S.; Marcarini, J. C.; de Souza, A. O.; de Paula, N. A.; Dorta, D. J.; Mantovani, M. S.; Ribeiro, L. R. Genistein at maximal physiologic serum levels induces G0/G1 arrest in MCF-7 and HB4a cells, but not apoptosis. *J. Med. Food* **2014**, *17* (2), 218–225.
- (61) Ercolano, G.; De Cicco, P.; Ianaro, A. New drugs from the sea: Pro-apoptotic activity of sponges and algae derived compounds. *Mar. Drugs* **2019**, *17* (1), 31.
- (62) Koh, M.; Lim, H.; Jin, H.; Kim, M.; Hong, Y.; Hwang, Y. K.; Woo, Y.; Kim, E.-S.; Kim, S. Y.; Kim, K. M.; et al. ANXA2 (annexin A2) is crucial to ATG7-mediated autophagy, leading to tumor aggressiveness in triple-negative breast cancer cells. *Autophagy* **2024**, *20* (3), 659–674.